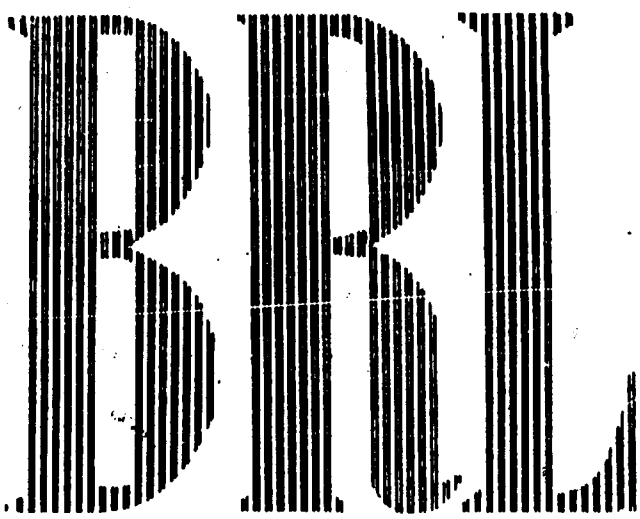


CATALOGED BY ASTIA  
AS AD NO. 298 293



MEMORANDUM REPORT NO. 1440  
OCTOBER 1962

DESIGN OF AIRCRAFT REVETMENTS

George A. Coulter  
Robert L. Peterson

298 293

ASTIA  
MAR 18 1963

BALLISTIC RESEARCH LABORATORIES

ABERDEEN PROVING GROUND, MARYLAND

REPRODUCED FROM  
BEST AVAILABLE COPY

NOTICE: When government or other drawings, specifications or other data are used for any purpose other than in connection with a definitely related government procurement operation, the U. S. Government thereby incurs no responsibility, nor any obligation whatsoever; and the fact that the Government may have formulated, furnished, or in any way supplied the said drawings, specifications, or other data is not to be regarded by implication or otherwise as in any manner licensing the holder or any other person or corporation, or conveying any rights or permission to manufacture, use or sell any patented invention that may in any way be related thereto.

ASTIA AVAILABILITY NOTICE

Qualified requestors may obtain copies of this report from ASTIA.

The findings in this report are not to be construed  
as an official Department of the Army position.

BALLISTIC RESEARCH LABORATORIES

MEMORANDUM REPORT NO. 1440

October 1962

DESIGN OF AIRCRAFT REVETMENTS

George A. Coulter  
Robert L. Peterson

Terminal Ballistics Laboratory

This research supported in part by the Defense Atomic Support Agency.  
WEB No. 01.007.

ABERDEEN PROVING GROUND, MARYLAND

BALLISTIC RESEARCH LABORATORIES

MEMORANDUM REPORT NO. 1440

GACoulter/RLPeterson/mec  
Aberdeen Proving Ground, Md.  
October 1962

DESIGN OF AIRCRAFT REVETMENTS

ABSTRACT

Air flow over two-dimensional model revetments, mounted in the 4 x 15 Inch Shock Tube, was traced by means of cigarette smoke grids photographed by a high speed framing camera. Tables of densities, flow speeds, and directions of flow, computed from the photographs, are given for an input shock wave of 8.3 psi average overpressure. Flow vectors are shown to illustrate the differences in the flow patterns for the different revetments tested.

## TABLE OF CONTENTS

	Page
LIST OF TABLES AND FIGURES . . . . .	6
LIST OF SYMBOLS . . . . .	7
1. INTRODUCTION . . . . .	9
2. DESCRIPTION OF THE APPARATUS . . . . .	10
2.1 General Description . . . . .	10
2.2 Camera Operation . . . . .	10
2.3 Smoke Generators . . . . .	13
2.4 Revetment Models . . . . .	14
3. DATA REDUCTION . . . . .	17
4. RESULTS AND APPLICATION . . . . .	24
4.1 Results . . . . .	24
4.2 Limitations . . . . .	46
4.3 Application . . . . .	46
5. DISCUSSION AND CONCLUSIONS . . . . .	55
5.1 Discussion . . . . .	55
5.2 Conclusions . . . . .	56
ACKNOWLEDGEMENT . . . . .	56
LIST OF REFERENCES . . . . .	57
APPENDIX A. TABLES FOR COMPARISON OF FLOW . . . . .	59

THIS  
PAGE  
IS  
MISSING  
IN  
ORIGINAL  
DOCUMENT

# LIST OF SYMBOLS

$C_D$	coefficient of drag
$C_L$	coefficient of lift
$C_M$	moment coefficient
$\bar{C}$	mean aerodynamic chord
$D$	drag parallel to air flow
$L$	lift perpendicular to air flow
$M$	pitching moment
$P_s$	free stream shock overpressure
$P'_s$	shock overpressure within the model
$q$	dynamic pressure
$q_2$	free stream dynamic pressure behind the shock wave
$T$	time, beginning when the free stream shock wave passed the inside, bottom edge of the upstream revetment
$\Delta T$	time between camera frames
$u$	flow speed
$u_2$	free stream flow speed behind the shock wave
$U$	free stream shock front speed
$W$	weight of aircraft
$x, y$	position coordinates measured from inside, bottom edge of upstream revetment
$\alpha$	angle of attack
$\theta$	flow deflection angle measured from horizontal
$\mu$	coefficient of static friction
$\rho$	density
$\rho_1$	ambient density ahead of the shock wave
$\rho_2$	free stream density behind the shock wave



## 1. INTRODUCTION

The present study of pressure and flow patterns in model revetments was undertaken to determine the design requirements for a revetment suitable for the protection of parked aircraft and semi-mobile missiles. Such design requirements are important to both the offensive and defensive planner. Information about aircraft protection by revetments is required by both the Air Force Intelligence and the Air Force, and Army Tactical Commands.

Previous experiments, Reference 1 - 5, with both laboratory shock waves and with field produced blast waves have shown that protection against drag-type damage is given by a shield placed upstream of the object to be protected. For purposes of comparative study, the dynamic pressure,  $1/2 \rho u^2$ , at a point behind the shield has been used as an indicator of the damage potential for given points within the flow field. The experiment described here is designed to measure the density,  $\rho$ , and the flow speed,  $u$ , for an input shock wave of constant pressure crossing a two-dimensional revetment model placed in the 4 x 15 inch shock tube.

The smoke stream technique, References 6 and 7, was modified by creating a grid from cigarette smoke. The smoke grid was used to trace the movement of the air flow past the model. The change in grid area as it moved with the flow indicated changes in density of the air flow.

This smoke technique was used with high speed photography which enabled both velocity vectors and density to be found for specified points within the model as a function of the travel time across the model. An illustration is given explaining how the flow patterns obtained by the smoke stream technique may be combined with a prior knowledge of the aerodynamic and vulnerability characteristics of a particular parked aircraft or missile to enable a prediction of its movement or damage to be made.

## 2. DESCRIPTION OF THE APPARATUS

### 2.1 General Description

A schematic of the apparatus is shown in Figure 1. The smoke generator and model revetment are shown separately below and are omitted from Figure 1 for purposes of clarity.

A conventional air-driven 4 x 15 inch shock tube, operated at an average ambient pre-shot pressure of 14.8 psi, was used for the experiment. Tracings of the characteristic shock waveforms are shown in Figure 2. About 1.1 msec, Figure 2-C, of the initial step portion of the shock wave was used to furnish data for the experiments. The input pressure was considered constant for the purposes of this experiment since the variation in waveform was small over this time interval.

The revetment model was mounted at the inside top of the test section to avoid pieces of "Mylar" diaphragm material from accumulating inside the model. The model is described in Section 2.4.

A Model 357 ASCOR Speedlight flash lamp was modified by attaching to it a reflecting cone with a small 0.1-inch diameter hole at the small end closed by a piece of glass from a frosted light bulb glued over the hole. This served as a sufficiently small point source for the 9-inch diameter collimating lens.

A high speed framing camera, Dynafax Model 326-3, was used to record the shock wave and the associated flow across the revetment model. The camera system was synchronized by a sequence timer which fired the shock tube and opened the camera shutter which was pre-set at 1/10 sec. The flash lamp was activated from a pressure transducer when the shock wave crossed its surface. The flash lamp duration was pre-set to coincide with one revolution of the camera film drum.

A shock wave velocity system and a frequency meter for the camera speed, completed the control equipment.

### 2.2 Camera Operation

Two difficulties arose during the use of the Dynafax camera. Optical alignment of the camera was difficult because of the internal diamond stops. The second problem was a mechanical one. The film would jam in the camera quite often when loading from the film cassette into the camera drum. This caused excess camera vibration, the film to shred, and camera misalignment.

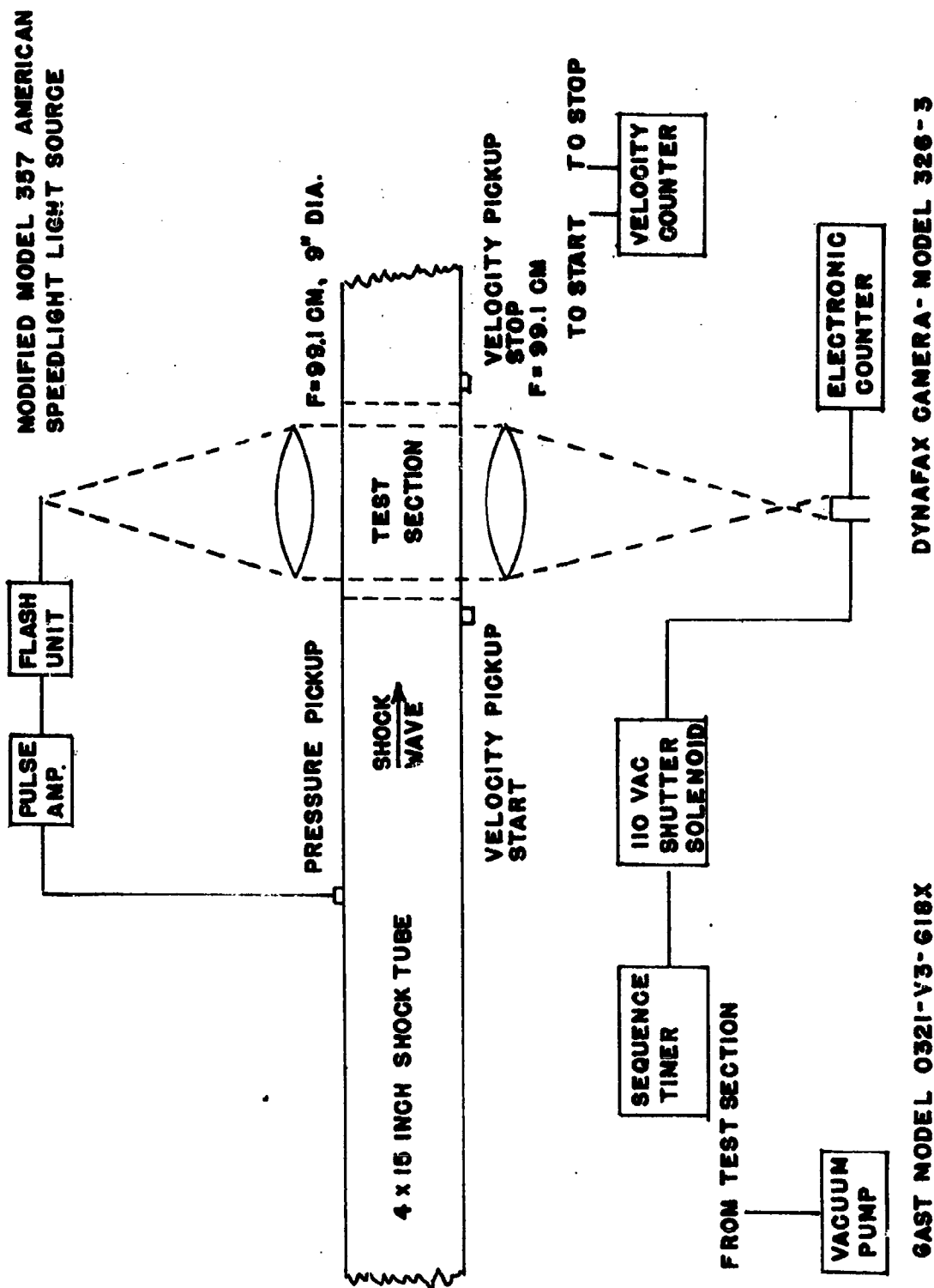


FIG. 1 EXPERIMENTAL APPARATUS

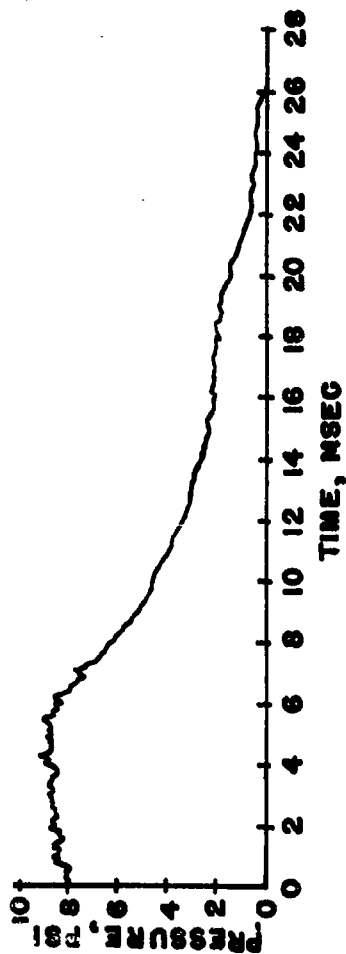


FIG. 2A-WAVEFORM 11.4 FEET UPSTREAM OF TEST SECTION

#### SHOCK PARAMETERS

$$P_2 = 8.0 \text{ PSI}$$

$$U = 1372 \text{ FT/SEC}$$

$$u_2 = 364 \text{ FT/SEC}$$

$$\rho_2 / \rho_1 = 1.36$$

$$\rho_1 = 0.00231 \text{ SLUGS/FT}^3$$

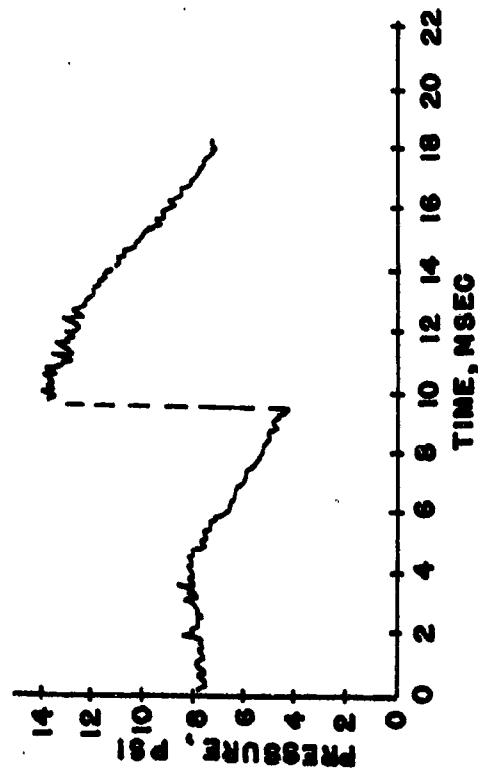


FIG. 2B-WAVEFORM AT TEST SECTION

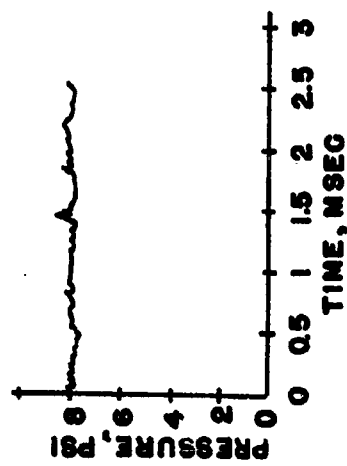


FIG. 2C-INITIAL PART OF WAVEFORM

FIG. 2 WAVEFORMS FROM THE 4 X 15 INCH SHOCK TUBE

The alignment was simplified by the use of a machined focusing tube, 11/16 inch long. A 3/32-inch hole was bored in the flat end plate of the focusing tube to allow the light beam to be centered.

For alignment, the focusing tube was threaded into the lens barrel. The image of the point source was focused on the plate of the focusing tube and adjusted to pass through the aligning hole in the end plate. The alignment was completed by placing a front surface mirror against the focusing plate and reflecting the light image back into the field lens to exactly fill it with light. A careful alignment was necessary in order to have well filled, uniformly illuminated film frames. For camera operation, the focusing tube was replaced with the light shield furnished for the camera lens. The film loading problem was alleviated by pulling the film into the cassette very tightly when it was loaded, and by putting a very tight reverse curl to the square film end. If the films were immediately loaded into the camera, jamming was kept to a minimum.

Sufficient light was obtained from the modified flash lamp described to allow Kodak Double - X film to be used. For frame exposures of 1.05  $\mu$ sec, it was necessary to process the film twice the recommended developing time in Ethol UFG film developer. Since only perforated Double - X film was available, a loss of information occurred whenever the image was at a perforation. Unperforated film would have increased the possible information area and also perhaps aided in the loading of the film cassette had the film been available.

### 2.3 Smoke Generators

Several methods and materials were tried in a search for a clean, dense, and easily produced smoke. Several materials were tried and discarded because of certain disadvantages they had. These are listed below:

1. "Dry ice",  $\text{CO}_2$ , had air blown over it; water condensed in the capillary smoke tubes.
2. Hydrochloric acid fumes were mixed with ammonia hydroxide; a solid precipitate formed in the capillary smoke tubes and closed them.
3. A smoke was made from wood pulp incense; water vapor condensed in the tubes.

4. Air was blown over hot SAE 20 motor oil; the smoke produced was not dense enough to photograph well.

5. An aerosol spray was made from "Flexol" (di-2 ethylhexylphthalate, DOP); it was not dense enough, even when dyed with an oil dye (Calco Red Z-1700). Cigarette smoke was superior in density, and photographed better, than any other "smoke" tested. Figure 3 shows the method used for production of the smoke streams which formed the grid used.

The streams were produced by a vacuum pump evenly "smoking" two cigarettes, one for each set of streams. Two flow valves were used to meter the very critical flow needed to maintain stable streams of smoke. Bypass valves were later installed around the metering valves in order to start the smoke quickly during the initial burning of the cigarettes; then, the bypass valves were closed. The metering valves then continued to maintain a steady flow of smoke suitable for photographing.

Too fast a flow, dirty capillary tubes, or touching smoke streams caused an unsteady flow of smoke. After careful adjustment a grid of vertical and horizontal streams, spaced 1/4 inch between the planes of the two sets, was maintained for long enough time to fire the shock tube and record the flow. This procedure was used for each repeated shot of the experiment.

#### 2.4 Revetment Models

A sketch of the basic type of model tested is shown in Figure 4 with an arrangement of the smoke grid obtained from the cigarette generators. The vertical streams were moved from position to position in order to observe the flow at different points inside the model as a function of time. During the latter stage of the experiment a four-stream grid was also used to lessen the total number of shots needed.

The model shown in Figure 4 is one of three tested. The three were chosen to illustrate the effects upon the air flow caused by changes in model shape, spacing, and orientation. The sloping models are adaptations of the basic shape given in Reference 7. A descriptive sketch for each is included in the corresponding data table below.

# CIGARETTE SMOKE GENERATORS

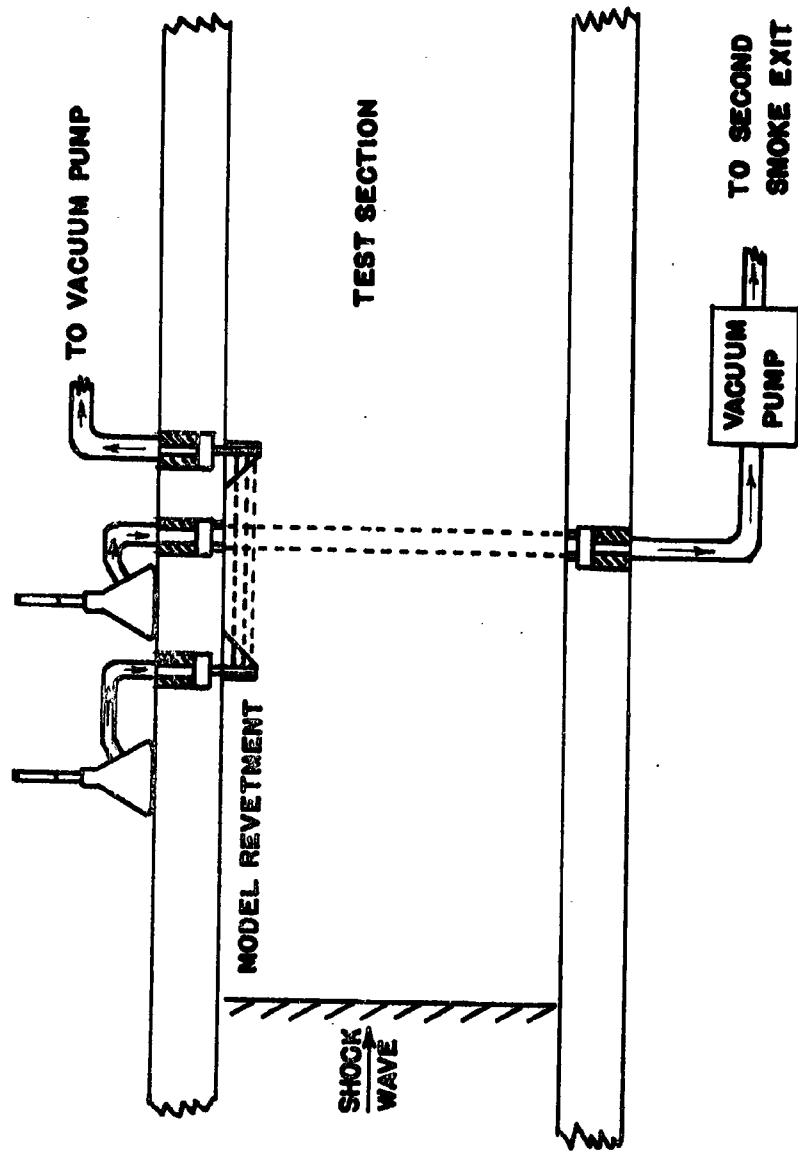
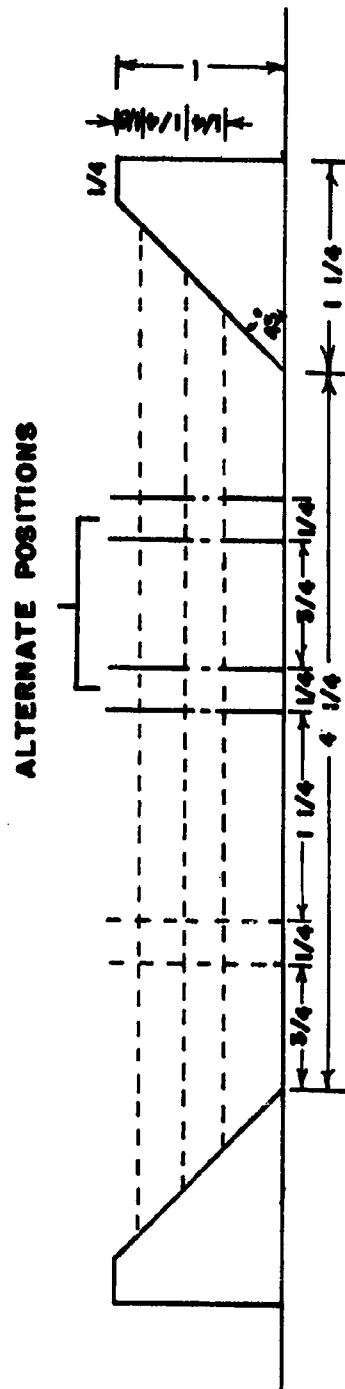


FIG. 3 SCHEMATIC ARRANGEMENT FOR PRODUCING THE SMOKE GRID



**FIG. 4 SMOKE GRID POSITIONS WITHIN THE REVETMENT MODEL**



### 3. DATA REDUCTION

The photographs of Figure 5 show the method of alternate framing on the film characteristic of the Dynafax camera. The pictures show the shock wave moving from left to right across the revetment models, causing the smoke grids to move with the air flow behind the shock wave.

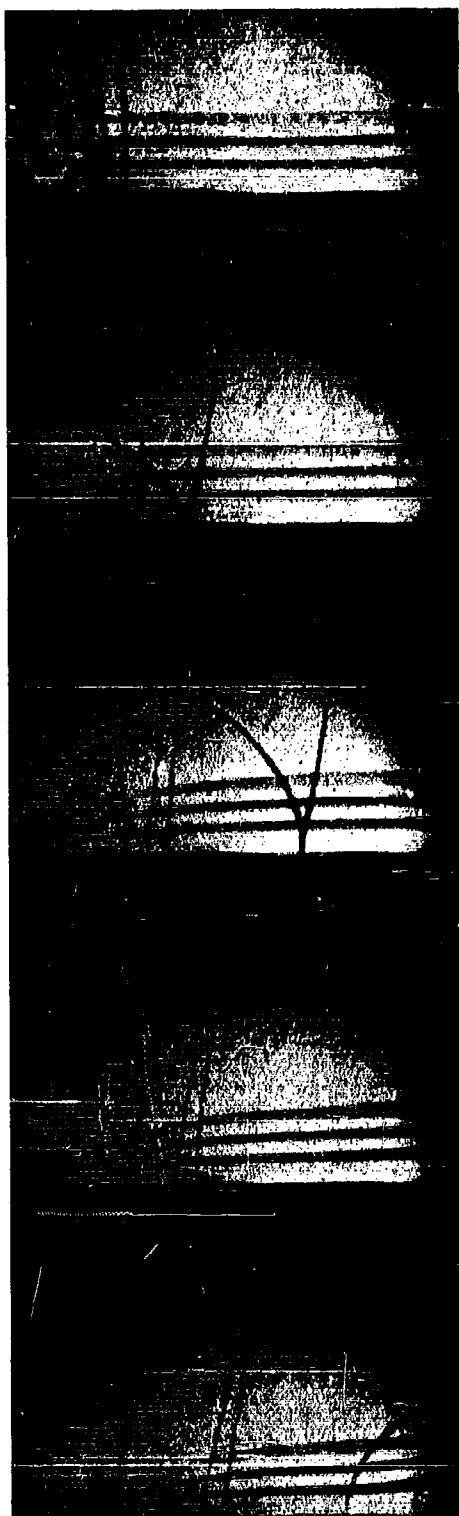
The data reduction was begun by assigning an arbitrary center of coordinates to a point at the inside bottom edge of the upstream part of the model. The smoke grid intersections were read by an optical film reader, using this coordinate system. From these coordinates, the distance of smoke grid travel and direction of travel were calculated from frame to frame. The distances in counts given from the reader were converted to actual distance by using the separation distance between the two parts of the model as a conversion scale. The distances of grid intersection travel were divided by the time between frames (obtained from the camera speed) to obtain an average flow speed. The average velocity vectors obtained in this way were assumed to have an origin located half-way in space and time between the two frames was used for the velocity calculation.

The times shown in Figure 5 were calculated from zero time beginning at the time the free stream shock wave appeared at a point over the coordinate system origin (the bottom inside edge of the upstream model) to the position shown by the given frame. The velocity of the free stream shock wave was obtained from a separate velocity system. This velocity and the distance of the shock wave from the coordinate origin (frame 1 of Figure 5A) allowed the initial frame time of  $T = 44 \mu\text{sec}$  to be calculated. Succeeding frame times were found by adding to the initial time the frame separation time,  $\Delta T$ , as found from the camera film drum speed.

Density at points behind the shock wave was found by comparing the flow of the disturbed smoke grid areas with the undisturbed pre-shot grids of the known density,  $\rho_1$ . The dynamic pressure,  $1/2 \rho u^2$ , could then be found from the density calculations and the flow speed assigned to the particular grid.

THIS  
PAGE  
IS  
MISSING  
IN  
ORIGINAL  
DOCUMENT

Fig. 5 Time Sequence of Shock Wave Crossing Revetment Models



Frame Number  
Time in  $\mu\text{sec}$

1	2
44	83
3	4
121	160
5	6
198	237
7	8
275	314
9	10
352	391

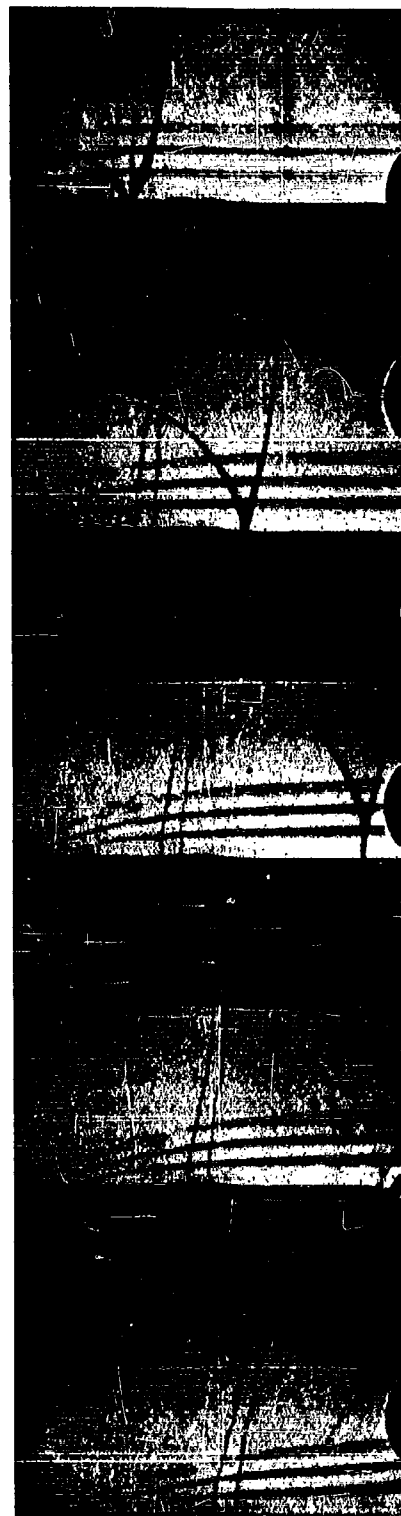
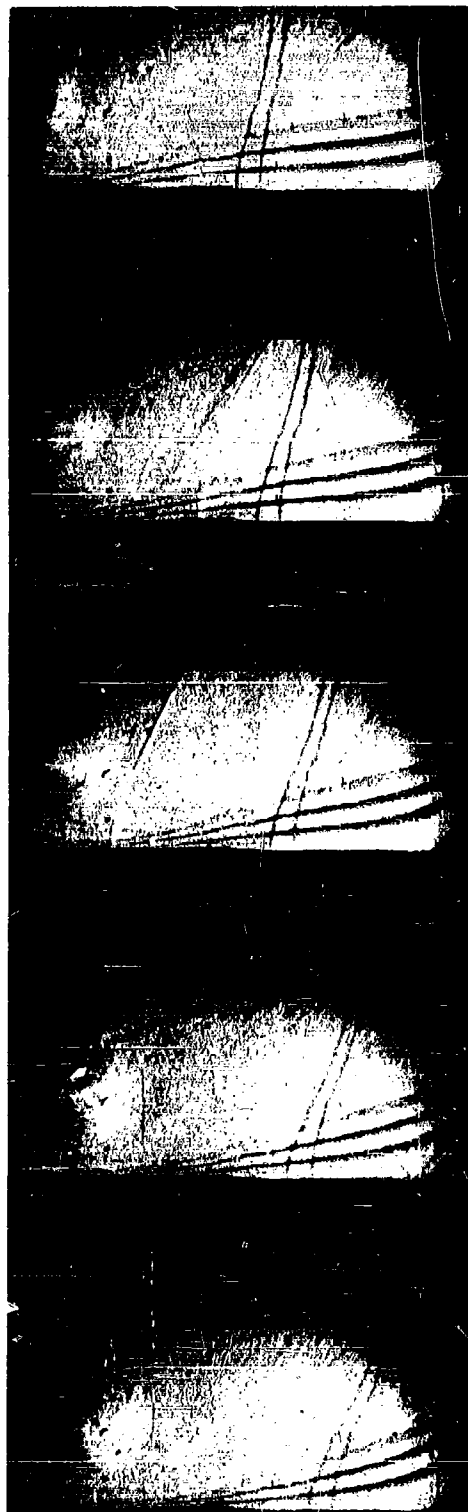


Fig. 5A Revetment with Inclined Interior Walls



Frame Number  
Time in usec

11	12
429	468

13	14
506	545

15	16
583	622

17	18
660	699

19	20
737	776

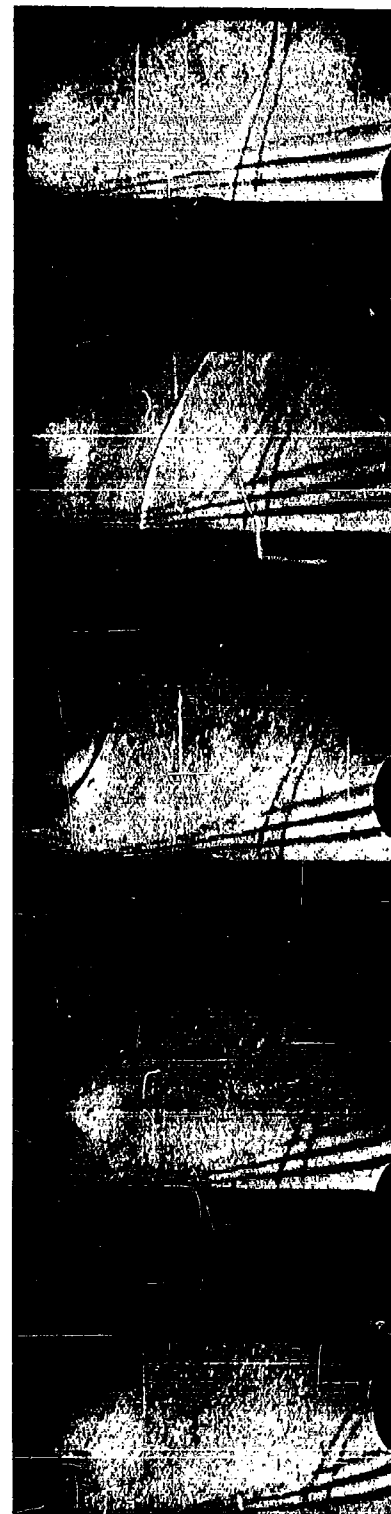


Fig. 5A (continued)

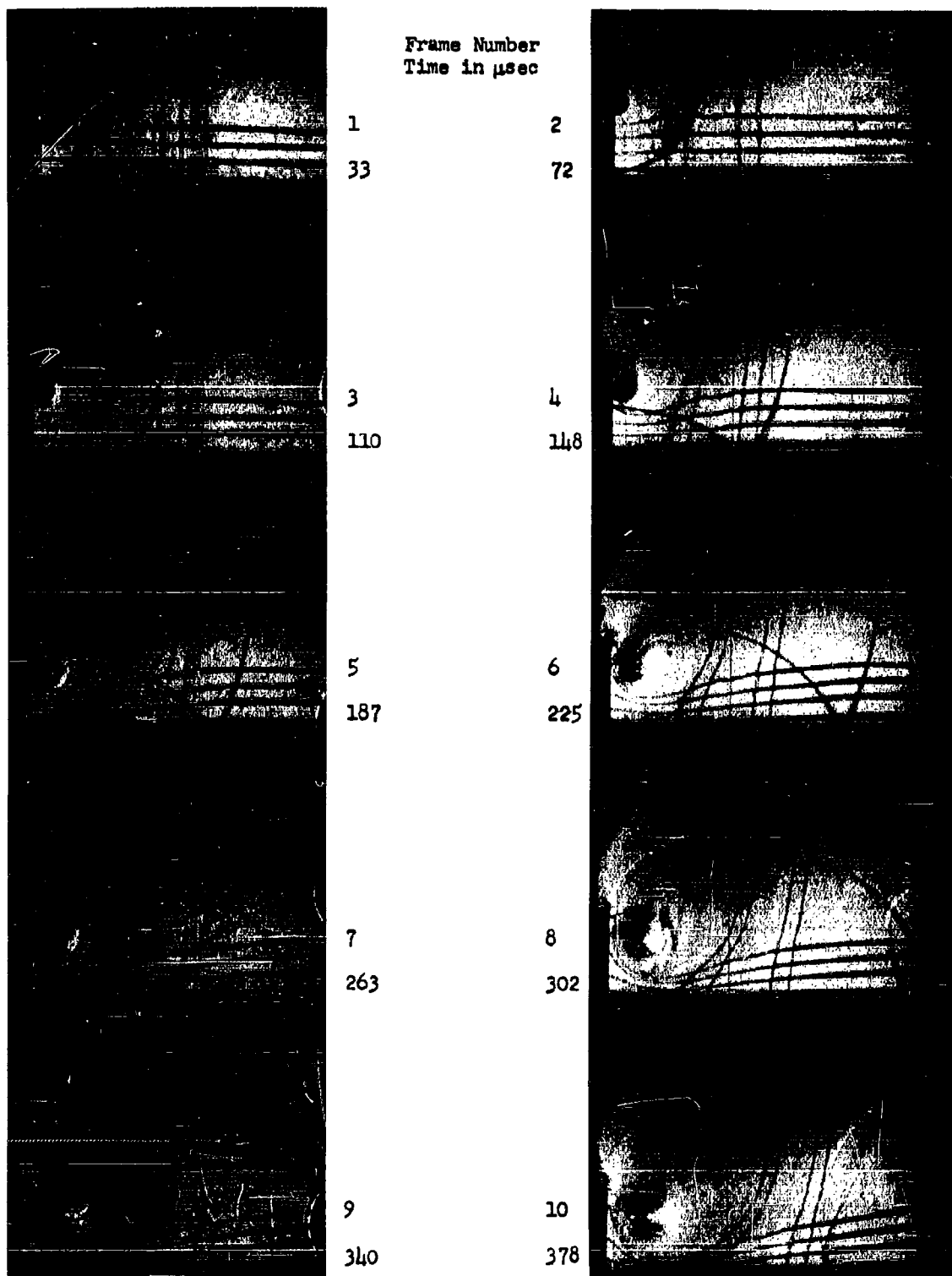
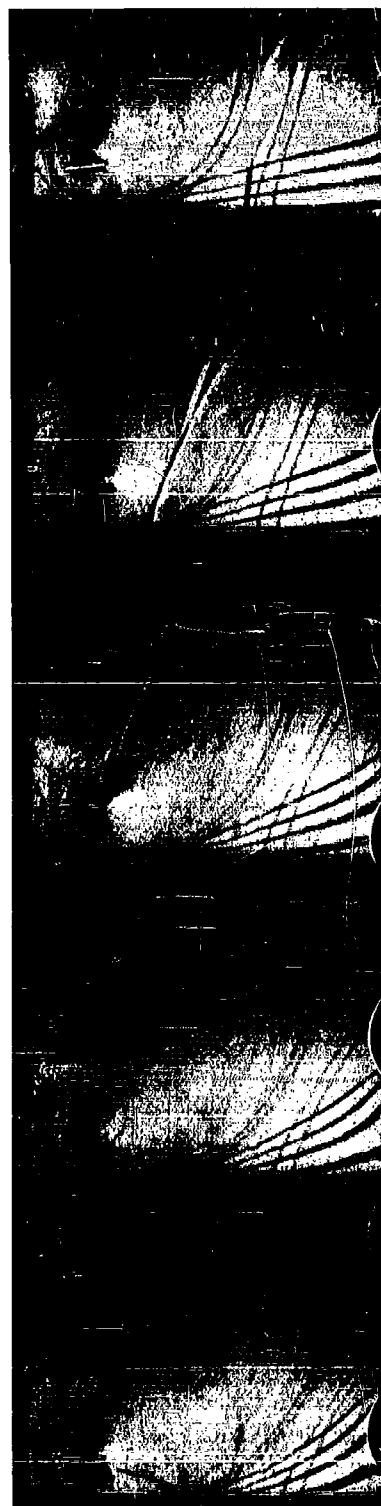


Fig. 5B Revetment with Vertical Interior Walls



Frame Number  
Time in  $\mu$ sec

11  
417

12  
455

13  
493

14  
532

15  
570

16  
608

17  
646

18  
685

19  
723

20  
762

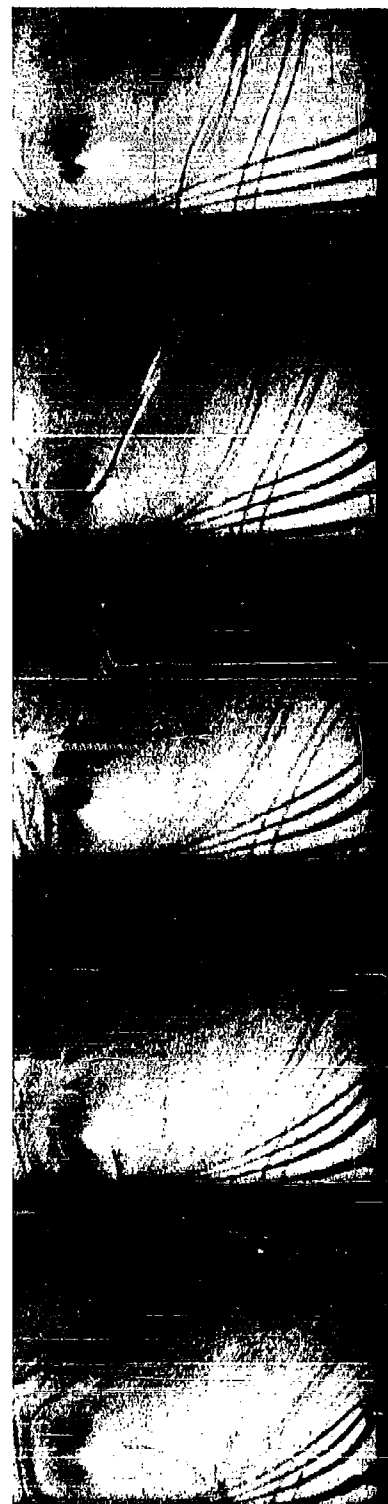


Fig. 5B (continued)

#### 4. RESULTS AND APPLICATION

##### 4.1 Results

The data from the present experiment are summarized in Tables I, II, and V. The data in Tables III and IV are rearranged from Reference 7 for comparison with the present data. Only data for times at which significant changes occurred are given in these tables. A more complete listing of the data is given in the tables presented in Appendix A.

Models I and III were of the same shape and spacing, but were oriented to the flow differently. Models I and II were oriented similarly but with different spacing. Model V was tested to show the effect of a vertical sided revetment.

One can see by comparing Figure 5 with the data tables that the flow regions, as a function of time, may be divided into roughly five intervals: an initial entrance phase; diffraction of the shock wave into the model; the downstream crossing with a regular reflection of the shock wave followed by a Mach stem growth in some cases; reflection of the shock wave from the downstream portion of the model back upstream into the flow; interaction of this reflection with the upstream vortex; and finally a region after the reflection expands out of the model. The same general divisions were found to apply to all the models tested.

A comparison of the flow is made in Figure 6. The vectors shown are taken from the complete tables in the Appendix. These values have a possible error of  $\pm 2$  percent for the magnitude of the flow and a direction error of  $\pm 6$  percent.

Set 1 of Figure 6 shows the contrast between the sloping interior wall and the straight wall of the model. Models I and II, Set 1A, show about the same flow pattern with a  $4^\circ$  to  $8^\circ$  downward inclination. The straight inside wall of Models III and V caused a steeper downward flow. Model III shows a flow speed of 27 to 44 ft/sec. Model V shows a range of flow speed between 131 to about 308 ft/sec as compared to 300 to 362 ft/sec for the sloping Models I and II.

Little change is seen for Models I, II, and III in Set 2 of Figure 6. Model V, however, exhibits a vortex action at the upstream end of the model which tends to rotate the flow downward and back upstream. The downstream end appears unaffected.



TABLE I. DATA FOR MODEL I

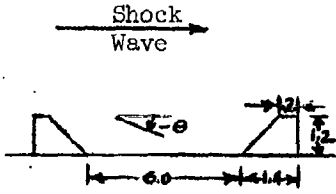
Time, $\mu$ sec	Position, in.		Flow Speed, ft/sec	Angle, deg	Density Ratio, $\rho/\rho_1$	Remarks
200	2.20	.34	314	-8.4	1.27	Model I
	2.27	.66	343	-5.6	1.26	
	2.39	.37	325	-6.2		
316	2.75	.34	353	-7.9	1.28	
	2.73	.65	354	-7.8	1.29	
	3.00	.35	380	-4.7		
	3.00	.67	405	-8.1		
548	3.67	.32	330	-4.0		Free Stream Shock Parameters $P_s = 8.3$ psi $u_2 = 375$ ft/sec $U = 1379$ ft/sec $\rho_1 = .00231$ slugs/ft <sup>3</sup> $P_1 = 14.8$ psi Reflection has passed smoke position.
	4.00	.34	281	-2.5		
	4.00	.66	305	-6.4		
	4.28	.63	335	-4.1		
625	3.96	.32	261	0.0		Minimum flow speed
	4.15	.34	292	0.0		
	4.20	.66	271	+2.5		
	4.53	.64	199	-7.2		
702	4.36	.32	205	-9.8		Flow increases again.
	4.36	.33	164	-8.4		
	4.40	.66	196	-5.6		
	4.69	.65	211	+1.1		
856	4.66	.33	297	0.0		Reflection is out of model.
	4.90	.37	303	+1.1		
	5.17	.65	295	-9.4		
1088	5.70	.24	184	-6.8		Reflection is out of model.
	4.25	.35	201	-14.4		
	5.05	.58	185	-14.7		

TABLE II. DATA FOR MODEL II

Time, $\mu$ sec	Position, in. x y		Flow Speed, ft/sec	Angle, deg	Density Ratio, $\rho/\rho_1$	Remarks
121	.90	.31	307	-7.1		Model II
	.92	.55	319	-11.5		
	.94	.79	328	-14.2		
	1.10	.33	302	-8.6	1.25	
	1.11	.56	308	-12.1	1.21	
	1.13	.84	318	-14.9	1.21	
160	1.06	.30	313	-5.6		Free Stream Shock Parameters
	1.08	.53	336	-7.9		
	1.12	.77	353	-5.8		$P_s = 8.3$ psi
	1.26	.32	334	-1.7	1.33	$u_2 = 375$ ft/sec
	1.29	.55	343	-6.2	1.31	$U = 1380$ ft/sec
	1.30	.80	352	-12.1	1.33	$\rho_1 = .00231$ slugs/ft <sup>3</sup>
						$P_1 = 14.8$ psi
275	1.49	.27	305	-2.0		
	1.52	.47	303	-6.2		
	1.56	.71	318	-8.1		
	1.72	.30	315	-4.4	1.35	
	1.73	.51	335	-5.2	1.53	Mach stem arrived at downstream model.
	1.76	.74	314	-3.5	1.41	Height of Mach stem is greater than smoke grid.
	2.67	.35	306	-3.2	1.44	
	2.68	.58	323	-3.1	1.43	
	2.68	.83	365	-3.1	1.18	
	3.45	.38	350	-3.6	1.21	
	3.45	.62	351	-3.9	1.24	
	3.45	.88	355	-5.4	1.18	
	3.64	.39	319	-2.7	1.21	
	3.64	.63	351	-3.5	1.24	
	3.63	.88	343	-3.3	1.23	

TABLE II. (CONTINUED) DATA FOR MODEL II

Time, $\mu$ sec	Position, in.		Flow Speed, ft/sec	Angle, deg	Density Ratio, $\rho/\rho_1$	Remarks
314	1.61	.26	309	-3.6		
	1.64	.47	308	-2.9		
	1.69	.69	320	-8.9		
	1.85	.28	313	-6.9	1.45	Mach stem reflects from downstream model. Reflection is traveling upstream.
	1.87	.49	324	-5.8	1.48	
	1.89	.75	322	+1.1	1.35	
	2.82	.34	325	-3.2	1.38	
	2.83	.57	325	-5.4	1.49	
	2.85	.82	337	-4.5	1.32	
	3.04	.34	328	-3.4	1.38	
	3.04	.58	318	-3.6	1.49	
	3.02	.82	342	-4.6	1.32	
	3.61	.38	347	+0.9	1.33	
	3.61	.61	357	+0.7	1.24	
	3.62	.85	385	-2.5	1.20	
	3.80	.38	336	+0.3	1.33	
391	1.91	.25	286	-1.6		
	1.94	.45	305	-4.6		
	2.00	.65	317	-6.5		
	2.16	.26	300	+2.0	1.41	
	2.18	.48	316	-1.9	1.44	
	2.21	.69	320	-10.2	1.44	
	3.15	.33	327	+1.3	1.69	
	3.17	.56	333	+2.9	1.68	
	3.16	.80	332	-0.2	1.48	
	3.36	.95	300	+2.7	1.69	
	3.36	.57	327	+2.9	1.68	
	3.37	.31	322	+3.1	1.48	
	3.88	.44	207	+9.1	1.39	
	3.90	.65	227	+13.7	1.44	
	4.06	.45	222	+19.9	1.39	

TABLE II. (CONTINUED) DATA FOR MODEL II

Time, $\mu$ sec	Position, in.		Flow Speed, ft/sec	Angle, deg	Density Ratio, $\rho/\rho_1$	Remarks
468	2.19	.22	250	- 4.5		
	2.21	.41	246	- 2.0		
	2.29	.64	263	- 4.7		
	2.42	.26	246	- 1.4	1.45	
	2.45	.46	239	- 0.3	1.59	
	2.50	.67	253	- 4.3	1.44	
	3.38	.36	202	+ 2.5	1.60	
	3.40	.58	255	+ 7.2	1.62	
	3.42	.83	247	+10.5	1.47	Reflection has passed smoke grid position.
	3.55	.37	188	+ 3.4	1.60	
	3.57	.60	214	+ 9.0	1.60	
	3.59	.86	251	+13.1	1.47	
	4.04	.45	198	+22.7	1.28	
	4.09	.72	249	+23.9	1.26	
	4.22	.51	191	+26.6	1.28	
	4.28	.77	259	+27.1	1.26	
583	2.45	.22	160	- 2.5		
	2.51	.40	175	- 3.0		
	2.58	.60	176	- 5.9		
	2.71	.26	164	- 1.8	1.42	Reflection begins to interact with vortex from upstream model. Flow speed becomes less at this time.
	2.74	.45	184	- 3.2	1.55	
	2.79	.67	200	- 3.0	1.45	
	3.67	.36	208	+15.3		
	3.72	.62	230	+16.5	1.38	
	3.77	.90	267	+13.6	1.42	
	3.86	.42	205	+12.2		
	3.90	.65	231	+16.9	1.38	
	3.99	.94	269	+18.0	1.42	

TABLE II. (CONTINUED) DATA FOR MODEL II

Time, $\mu$ sec	Position, in. x y		Flow Speed, ft/sec	Angle, deg	Density Ratio, $\rho/\rho_1$	Remarks
660	2.64	.21	254	-3.4		
	2.70	.39	247	-2.7		
	2.78	.58	249	-1.3		
	2.92	.25	254	-3.3	1.47	
	2.95	.45	254	-3.5	1.38	
	3.00	.64	251	-3.3	1.36	
	3.87	.41	234	+7.0		
	3.97	.69	274	+11.8	1.34	
	3.99	.95	282	+11.7		
	4.07	.47	238	+16.9		
	4.15	.73	290	+18.5		
	4.20	1.03	345	+16.6	1.34	
853	3.22	.19	194	-1.7		Upstream reflection is out of model completely.
	3.29	.37	200	-0.9		
	3.40	.55	225	+2.1		
	3.51	.24	200	-2.8	1.45	
	3.54	.44	203	+0.9	1.39	
	3.64	.66	236	+13.4	1.31	
1084	3.82	.20	173	+1.3		Vortex has lost distinction by this time.
	3.90	.42	233	+13.3		
	4.06	.63	249	+13.1		
	4.07	.33	211	+16.1		
	4.15	.54	260	+21.6		
	4.31	.79	218	+4.0		

TABLE III. DATA FOR MODEL III

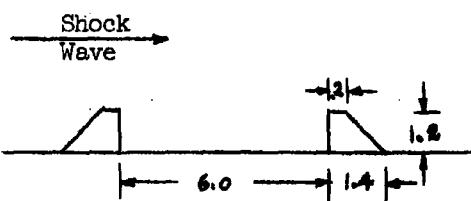
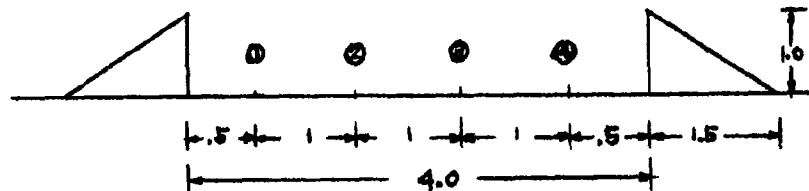
Time, μ sec	Position, in.		Flow Speed, ft/sec	Angle, deg	Remarks
x	y				
205	3.00	.90	27	-63	Model III
	3.00	1.12	44	-36	
244	2.60	.32	48	-11	 <p>Note: Data taken from Teel, Ref. 7</p>
	2.60	.75	117	-36	
	2.60	.95	187	-51	
267	2.50	.95	395	-24	<p>Free stream Shock Parameters</p> <p><math>P_s = 8.0</math> psi</p> <p><math>u_2 = 365</math> ft/sec</p> <p><math>U = 1375</math> ft/sec</p> <p><math>\rho_1 = .00231</math> slugs/ft<sup>3</sup></p> <p><math>P_1 = 14.8</math> psi</p>
	3.05	.35	287	-7	
	3.05	.77	310	-6	
	3.08	1.10	350	-21	
329	3.30	.34	389	-5	<p>Note: Density measurements not taken.</p>
	3.40	.77	371	-9	
	3.50	1.10	403	-19	
391	3.55	.32	299	-7	
	3.55	.75	329	-13	
431	3.40	.30	379	-9	
	3.40	.72	392	-10	
	3.30	.90	388	-20	
617	4.00	.30	263	-7	
	4.02	.62	260	-5	

TABLE IV. DATA FOR MODEL IV

Time, $\mu$ sec	Position (1)		Position (2)		Position (3)		Position (4)		Remarks
	$\rho/\rho_1$	$P'_s$	$\rho/\rho_1$	$P'_s$	$\rho/\rho_1$	$P'_s$	$\rho/\rho_1$	$P'_s$	
196	1.22	4.9	1.24	5.3	1.00	0	1.00	0	
252	1.19	4.1	1.30	6.6	1.32	6.7	1.00	0	
311	1.23	5.0	1.30	6.6	1.31	6.4	1.30	6.2	
337	1.23	5.0	1.33	7.5	1.34	7.2	1.33	7.0	Note: Data from Ref. 7, Appendix B
379	1.14	3.3	1.24	5.4	1.25	5.3	1.60	12.9	
430	1.14	3.0	1.28	6.2	1.57	12.5	1.48	10.3	Reflection in middle of model space.
492	1.25	5.6	1.53	12.3	1.48	10.3	1.45	9.5	
602	1.38	8.6	1.42	9.5	1.44	9.3	1.44	9.3	Reflection inter- acting with up- stream vortex
716	1.28	6.4	1.40	9.1	1.39	8.2	1.38	8.0	
830	1.32	7.1	1.28	6.2	1.36	7.6	1.46	9.9	
1066	1.29	6.4	1.21	4.7	1.34	7.2	1.37	7.8	
1349	1.40	9.0	1.29	6.4	1.40	8.4	1.46	9.9	Reflection out of the model.
1629	1.35	7.6	1.28	6.2	1.40	7.2	1.40	8.5	

Model IV

Shock Wave

Free stream shock  
Parameters

$$P'_s = 8.3 \text{ psi}$$

$$u_2 = 375 \text{ ft/sec}$$

$$U = 1379 \text{ ft/sec}$$

$$\rho_1 = .00231 \text{ slugs/ft}^3$$

$$P_1 = 14.8 \text{ psi}$$

TABLE V. DATA FOR MODEL V

Time, $\mu$ sec	Position, in. x y	Flow Speed, ft/sec	Angle, deg	Density Ratio, $\rho/\rho_1$	Remarks
110	.73 .38	177	-42.7	1.13	Model V
	.77 .59	236	-52.9	1.12	
	.81 .81	296	-48.1	1.13	Shock Wave
	1.03 .65	219	-48.3	1.12	
	1.06 .88	251	-44.4	1.13	
148	.79 .15	144	-40.2	1.39	Free Stream Shock Parameters
	.80 .32	181	-46.9	1.39	$P_s = 8.6$ psi
	.83 .50	233	-44.3	1.26	$u_2 = 385$ ft/sec
	.90 .71	298	-53.3	1.22	$U = 1392$ ft/sec
	1.04 .15	164	-18.1	1.39	$\rho_1 = .00231$ slug/ft <sup>3</sup>
	1.07 .36	208	-34.2	1.39	$P_1 = 14.7$ psi
	1.11 .56	246	-39.2	1.26	
	1.15 .80	306	-42.7	1.22	Shock wave is about midway across model.
	1.73 .20	138	-15.0	1.14	
	1.75 .45	194	-33.2	1.11	
	1.76 .68	221	-38.2	1.20	
	1.79 .91	244	-31.4	1.22	
	1.98 .21	102	-24.0	1.14	
	1.99 .48	146	-38.1	1.11	
	2.00 .70	154	-32.2	1.20	
263	.95 .08	91	-29.1	1.99	
	.96 .19	103	-10.6	1.49	
	1.02 .32	154	-30.7	1.30	
	1.16 .48	196	-66.6	1.27	
	1.54 .14	224	-13.4	1.79	
	1.56 .33	246	-14.3	1.35	
	1.59 .49	258	-12.5	1.43	
	1.64 .70	282	-16.6	1.23	
	2.09 .15	286	+3.1	1.50	

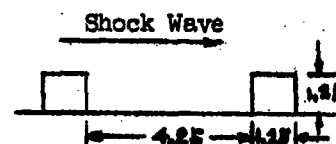




TABLE V. (CONTINUED) DATA FOR MODEL V

Time, $\mu$ sec	Position, in.		Flow Speed, ft/sec	Angle, deg	Density Ratio, $\rho/\rho_1$	Remarks
x	y					
	2.12	.34	298	+1.7	1.44	
	2.14	.54	312	-6.4	1.45	
	2.66	.23	303	-3.5	1.35	
	2.66	.48	293	-10.9	1.42	
	2.67	.66	294	-9.0	1.47	
	2.69	.89	297	-12.2	1.20	
	3.06	.19	256	-3.0	1.32	
	3.07	.47	272	-10.6	1.27	
	3.07	.67	261	-11.0	1.42	
	3.09	.90	280	-15.4	1.15	
302	.97	.07	45	-76.0	1.90	Shock wave has reflected from downstream part of model.
	.99	.19	93	-76.9	1.34	
	1.07	.29	129	-64.2	1.43	
	1.19	.42	174	-50.0	1.33	
	1.62	.13	196	-9.0	1.59	
	1.66	.30	234	-13.6	1.33	
	1.70	.47	288	-14.5	1.41	
	1.77	.66	292	-19.6	1.29	
	2.22	.16	285	-13.1	1.48	
	2.24	.35	281	-7.6	1.47	
	2.27	.53	289	-10.7	1.45	
	2.30	.75	312	-13.7	1.33	
	2.80	.22	326	-8.0	1.36	
	2.81	.45	341	-4.4	1.34	
	2.81	.64	324	-3.8	1.35	
	2.82	.87	322	-12.2	1.30	
	3.39	.21	324	-13.4	1.36	
	3.40	.46	325	-4.5	1.37	
	3.40	.66	315	-3.3	1.31	
	3.48	.89	321	-7.9	1.32	

TABLE V. (CONTINUED) DATA FOR MODEL V

Time, $\mu$ sec	Position, in.		Flow Speed, ft/sec	Angle, deg	Density Ratio $\rho/\rho_1$	Remarks
	x	y				
455	2.03	.09	140	-5.4	1.66	Mach reflection has formed from downstream reflection and is above the middle of the model.
	2.08	.21	135	-13.2	1.47	
	2.17	.35	148	-9.9	1.57	
	2.25	.51	166	-2.0	1.46	
	2.82	.15	68	-8.5	1.95	
	2.85	.35	80	-18.4	1.61	
	2.90	.54	95	-14.0	1.62	
	2.95	.74	101	+11.3	1.59	
	3.51	.20	61	+37.6	1.59	
	3.54	.47	95	+47.7	1.77	
	3.58	.70	134	+50.4	1.68	
	3.63	.94	178	+44.1	1.49	
	3.82	.23	61	+67.6	1.63	
	3.84	.53	123	+66.6	1.50	
	3.87	.78	174	+63.4	1.50	
	3.94	1.05	244	+56.3	1.61	
570	2.07	.07	41	-14.0	1.96	Mach stem reflection has interacted with vortex.
	2.16	.19	72	-73.3	1.50	
	2.25	.31	75	+90.0	1.61	
	2.35	.46	124	0.0	1.59	
	2.71	.11	128	0.0	1.90	
	2.75	.30	124	-1.4	1.51	
	2.81	.47	150	-1.3	1.60	
	2.89	.68	162	+2.2	1.45	
	3.32	.24	101	+10.8	1.58	
	3.36	.51	127	+4.4	1.53	
	3.42	.72	151	+27.6	1.54	
	3.47	.96	171	+29.2	1.43	
	3.59	.26	84	+16.5	1.46	
	3.66	.59	135	+31.0	1.72	
	3.72	.86	175	+31.6	1.60	
	3.82	1.14	273	+40.5	1.52	

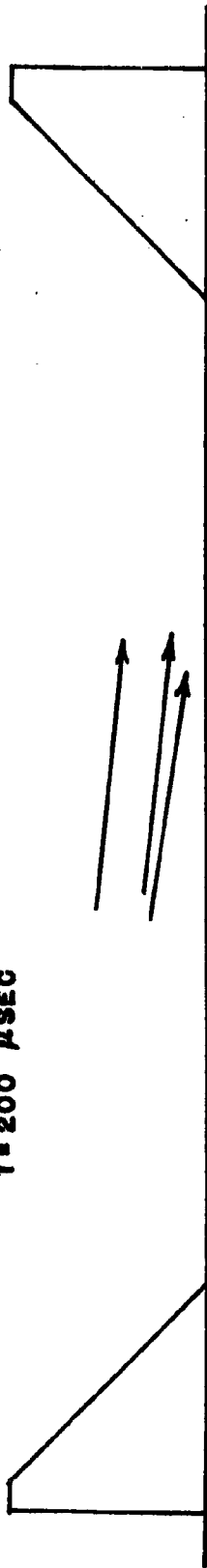
TABLE V. (CONTINUED) DATA FOR MODEL V

Time, $\mu$ sec	Position, in.		Flow Speed, ft/sec	Angle, deg	Density Ratio, $\rho/\rho_1$	Remarks
x	y					
646	2.12	.05	61	+7.6	2.02	Small portion of Mach stem has reflected from up- stream wall.
	2.20	.15	58	-6.3	1.46	
	2.31	.28	94	-45.0	1.47	
	2.47	.45	102	-46.7	1.42	
	2.83	.10	142	+4.1	1.95	
	2.89	.27	150	+11.9	1.60	
	2.98	.47	158	-4.1	1.54	
	3.08	.69	171	-17.9	1.48	
	3.41	.24	129	+36.2	1.63	
	3.50	.54	162	+31.0	1.40	
	3.55	.77	188	+36.2	1.48	
	3.65	1.05	247	+40.2	1.44	
	3.68	.30	109	+31.8	1.30	
	3.76	.65	118	+42.3	1.64	
	3.86	.98	168	+34.2	1.57	
	4.00	1.30	242	+39.2	1.43	
838	3.15	.12	143	+2.7	1.76	Vortex has become indistinct.
	3.18	.28	167	+14.9	1.54	
	3.32	.50	165	+6.8	1.59	
	3.46	.77	191	+8.1	1.33	
	3.38	.18	168	+15.4	1.76	
	3.44	.42	170	+18.8	1.55	
	3.57	.67	236	+31.7	1.59	
	3.73	1.00	257	+39.8	1.33	

SET 1A

VECTOR SCALE: 1 INCH = 200 FT/SEC

T = 200  $\mu$ SEC



I

T = 198  $\mu$ SEC



II

FIG. 6 COMPARISON OF FLOW VECTORS

VECTOR SCALE: 1 INCH = 200 FT/SEC

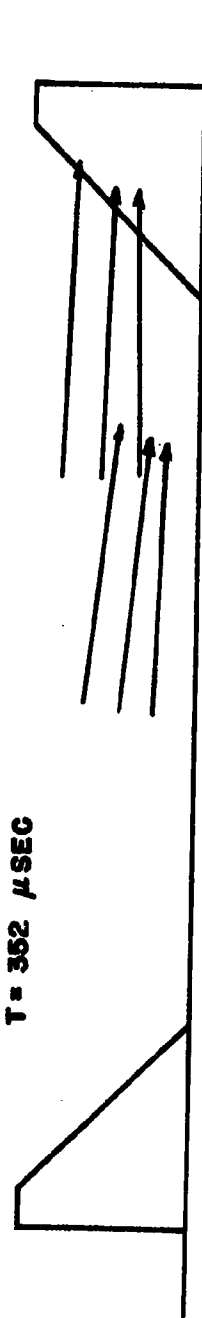
T = 355  $\mu$ SEC

SET 2A



I

T = 352  $\mu$ SEC

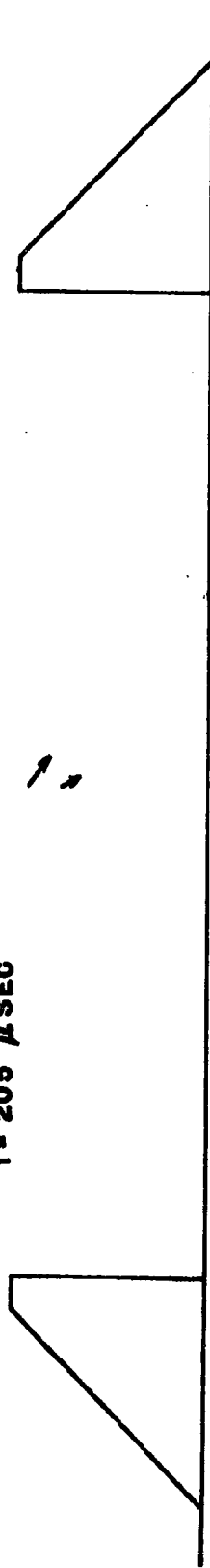


II

FIG. 6 (CONTINUED) COMPARISON OF FLOW VECTORS

VECTOR SCALE: 1 INCH=200 FT/SEC SET 1B

T = 205  $\mu$ SEC



III

T = 187  $\mu$ SEC

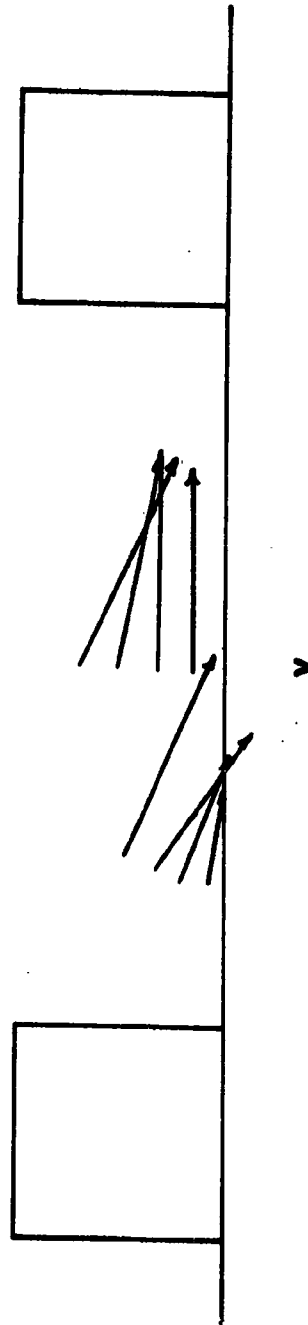
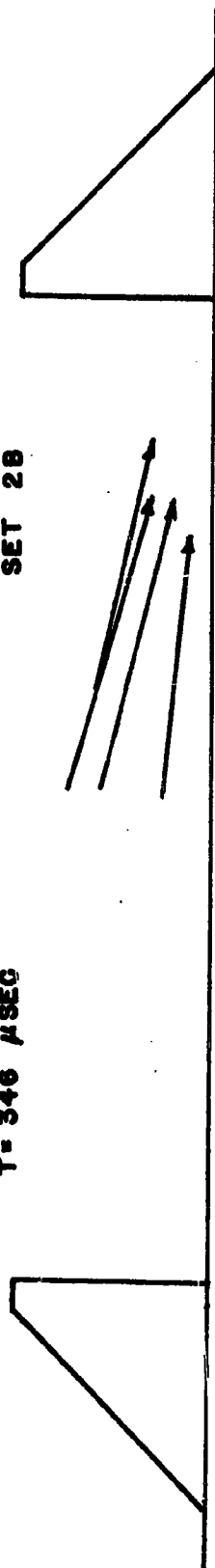


FIG. 6 (CONTINUED) COMPARISON OF FLOW VECTORS

VECTOR SCALE: 1 INCH=200 FT/SEC

T = 346  $\mu$ SEC

SET 2B



III

T = 340  $\mu$ SEC

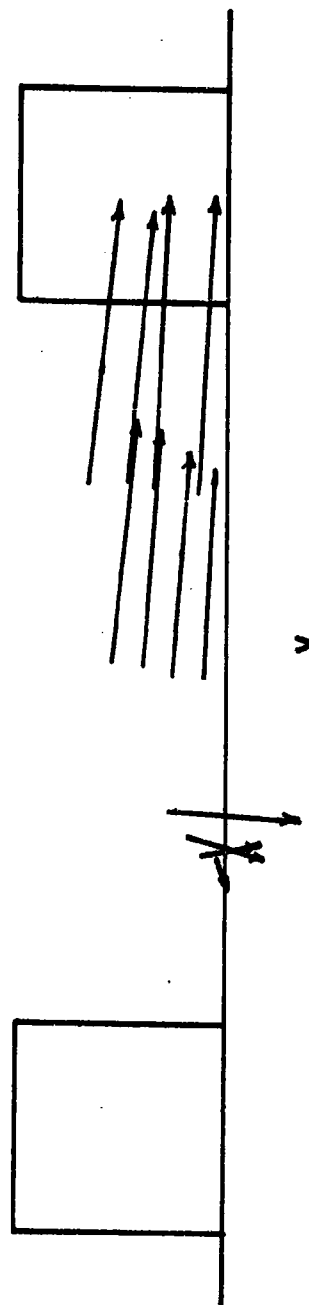


FIG. 6 (CONTINUED) COMPARISON OF FLOW VECTORS

The third set of Figure 6 exhibits several changes from the previous time regions. Model I still shows about the same flow; however, the reflection from downstream has passed the observation position for Model II. This caused the flow of 350 to 360 ft/sec at the previous time to be changed to 160 to 200 ft/sec and also it caused an upward flow near the downstream end of the model. Model III still exhibits downward flows of 284 to 330 ft/sec at an inclination of 3 to 21°. Model V also shows a similar change to Model II since the reflection has also passed the smoke grid. This caused the flow speed to become less and also gave it a positive direction at the downstream end of the model. The measured flow speed ranged from 36.5 to about 300 ft/sec near the top of the downstream level.

Set 4 illustrates the reflected region of flow for all the models. The flow magnitudes are similar, except for Model V which is smaller. Model III differs in that the flow direction is still downward towards the floor of the model. The last set of Figure 6 shows an erratic behavior for Model I. This seems to be the result of the reflection moving out of the model and the vortex change. Model II sustains the upward flow.

Some insight about the density within the models may be obtained from a study of the above Tables I, II, IV, and V. Table IV is included because of a model similarity to that of Model III. The following density pattern was found to be present within the models. A density ratio,  $\rho / \rho_1$ , of between 1.14 and 1.23 was found for region (1), Model IV, for times 196 to 430 usec. For region (3), a ratio of 1.57 was observed for a time just after the reflected wave moved upstream past the observation point. Data from Table II, for Model II, show a somewhat higher ratio of 1.62 for this region. The side-on pressure,  $P_s$ , from Table IV, shows a corresponding increase as the reflection passed. Table V shows the density ratio increased to about 2. This value exceeds the value of 1.83 for a normally reflected wave and is probably caused by the Mach reflection which appears to take the place of a regular reflection. Approximately a free stream density ratio of 1.4 occurs at later times, although, Model V shows erratic density behavior throughout.

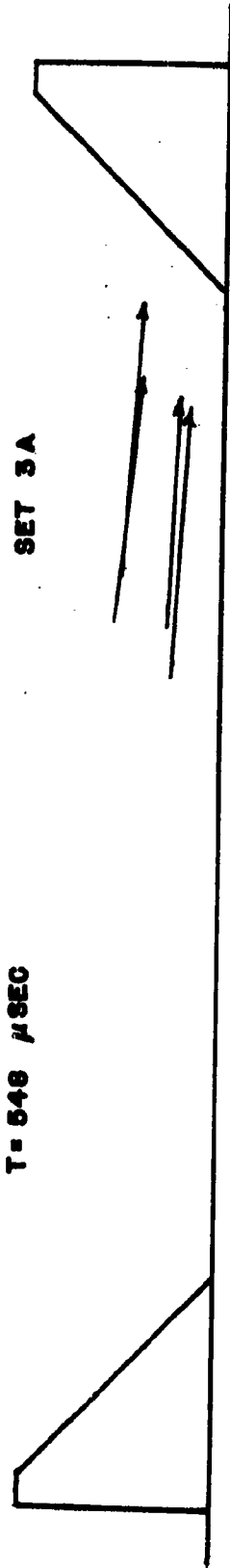
The values of density ratio,  $\rho / \rho_1$ , are accurate to about  $\pm 5$  percent.



VECTOR SCALE: 1 INCH = 200 FT/SEC

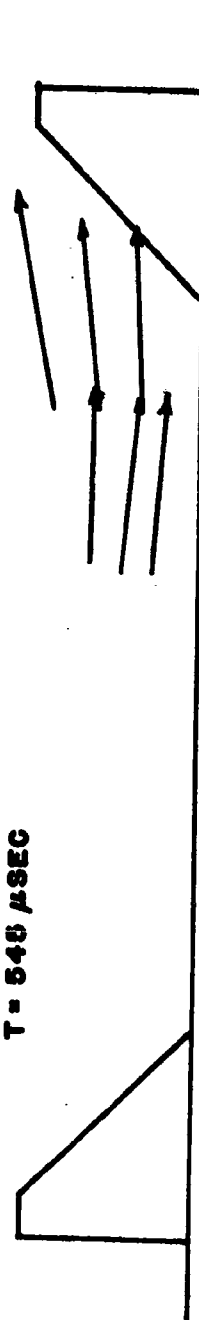
T = 548  $\mu$ SEC

SET 3A



I

T = 548  $\mu$ SEC



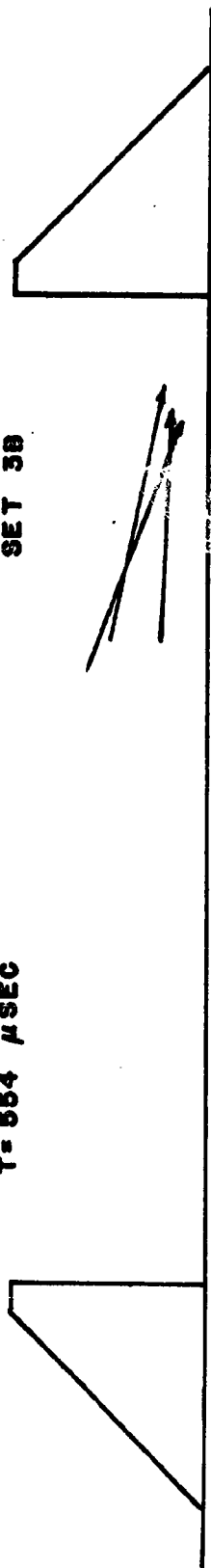
II

FIG. 6 (CONTINUED) COMPARISON OF FLOW VECTORS

VECTOR SCALE: 1 INCH = 200 FT/SEC

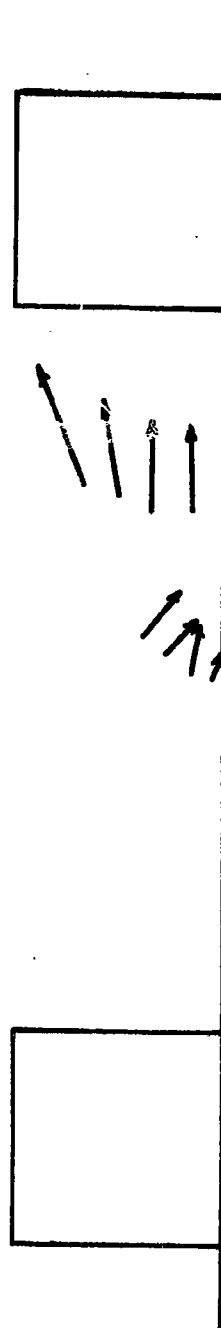
T = 554  $\mu$ SEC

SET 3B



III

T = 532  $\mu$ SEC



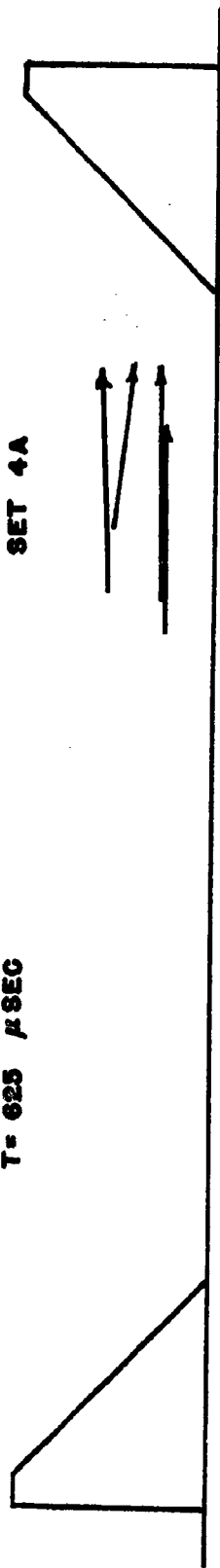
V

FIG. 6 (CONTINUED) COMPARISON OF FLOW VECTORS

VECTOR SCALE: 1 INCH = 200 FT/SEC

T = 625  $\mu$ SEC

SET 4A



1

T = 622  $\mu$ SEC



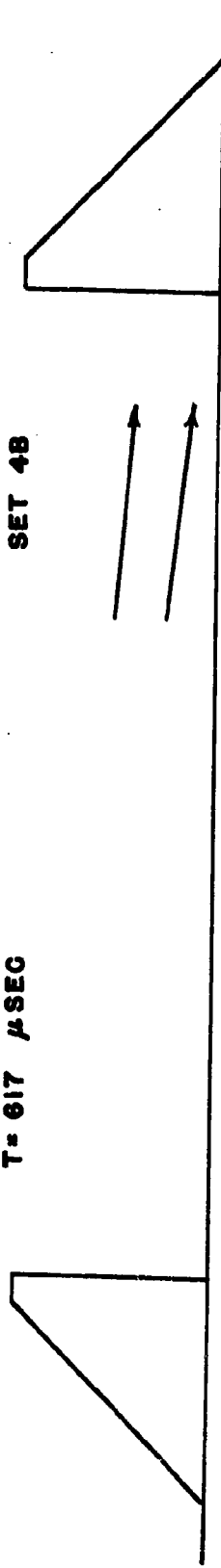
11

FIG. 6 (CONTINUED) COMPARISON OF FLOW VECTORS

VECTOR SCALE: 1 INCH = 200 FT/SEC

T = 617  $\mu$ SEC

SET 4B



III

T = 608  $\mu$ SEC



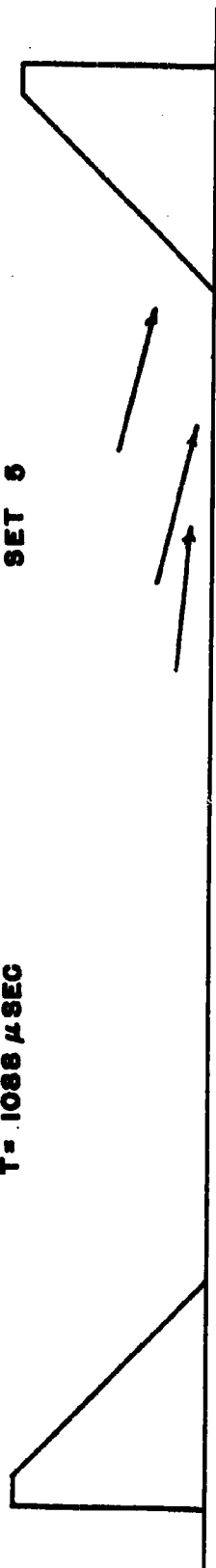
V

FIG. 6 (CONTINUED) COMPARISON OF FLOW VECTORS

VECTOR SCALE: 1 INCH = 200 FT/SEC

T = 1088  $\mu$ SEC

SET 8



I

T = 1084  $\mu$ SEC



II

FIG. 6 (CONTINUED) COMPARISON OF FLOW VECTORS

#### 4.2 Limitations

The present experimental data were limited to those obtained from two-dimensional models. The same general trends, however, ought to apply for a three-dimensional case. For example, Reference 8 gives the side-on pressure for three positions across the floor of a circular revetment with a cross-section similar in shape to Models I and II. Figure 7 shows part of the pressure-time traces reproduced from Reference 8 for comparison with the present data.

For  $0^\circ$  orientation, reflections appeared on the traces for about one-half millisecond of time to cause a pressure higher than that of the input wave. After this time the pressure came back to the input level, then decayed below that level. In the  $270^\circ$  orientation, only the position nearest a wall showed the reflection to any extent.

This work indicates a trend, at least in pressure, similar to that observed for the two-dimensional case.

#### 4.3 Application

The data may be applied to a specific example in the following manner. For long revetment walls, the present two-dimensional data may be used. For example, Model II, may be scaled to full size to meet the needs of a particular aircraft. For this application data for the F-105D is used. Aerodynamic data for a  $1/4$ -scale model test of the F-105, References 9 and 10 will be used for the present discussion.

For the revetment to accommodate the F-105D, it is necessary to scale the size of the revetment model up in size about 250 times. The dimensions of the full size revetment are shown in Figure 8 with the schematic position of the wing and horizontal tail. Only flow from the head-on ( $0^\circ$  yaw) orientation will be considered here.

The revetment should be designed large enough to keep the aircraft out of the vortex from the upstream wall and also out of the positive, upward flow at the sloping downstream wall. The schematic wing and tail positions in Figure 8 satisfy these requirements. The distances from the walls are equal to about one revetment wall height.

REF: R.O. CLARK. BRL TECH. NOTE  
983,AFSWP 776, JAN, 1955.

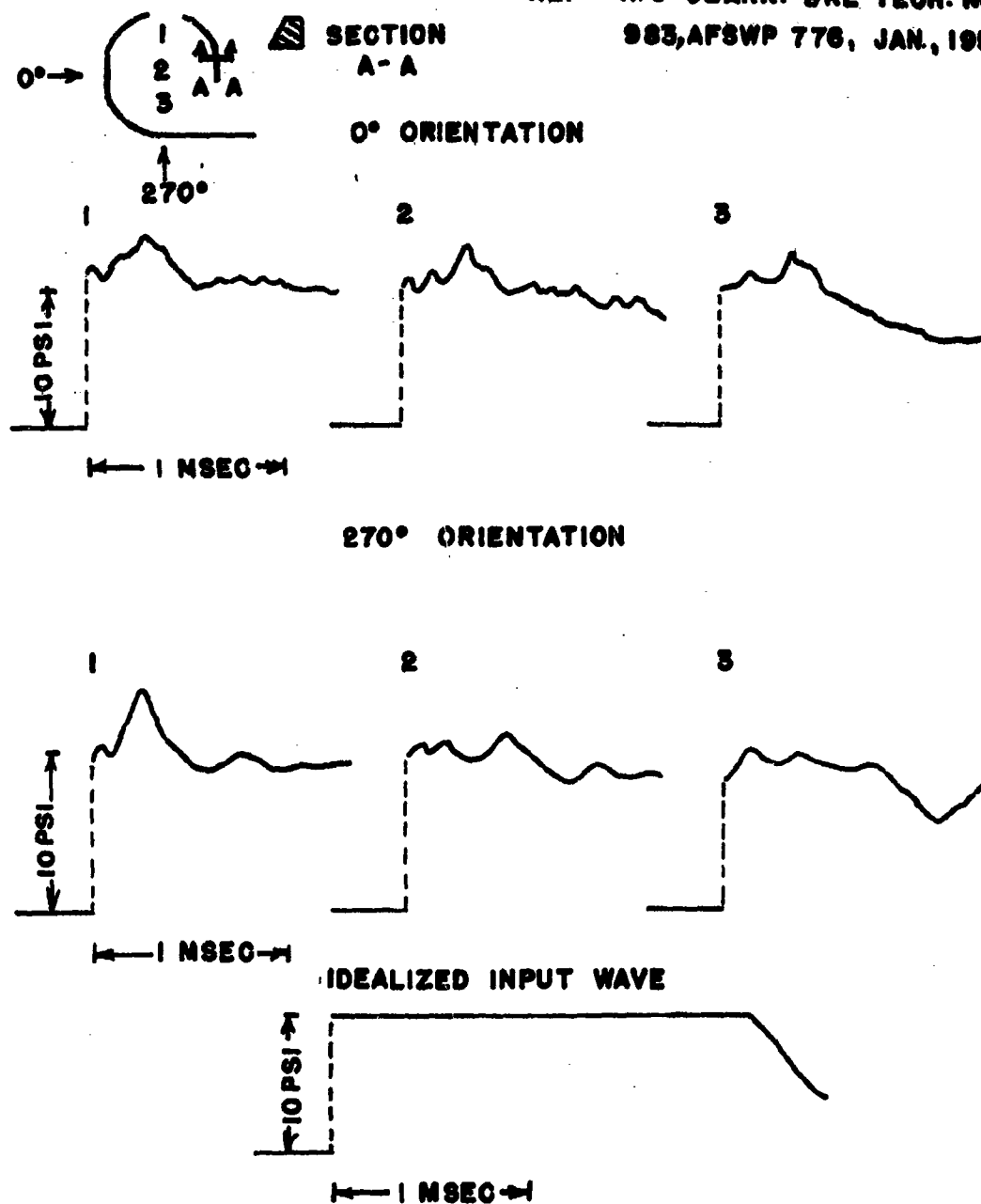
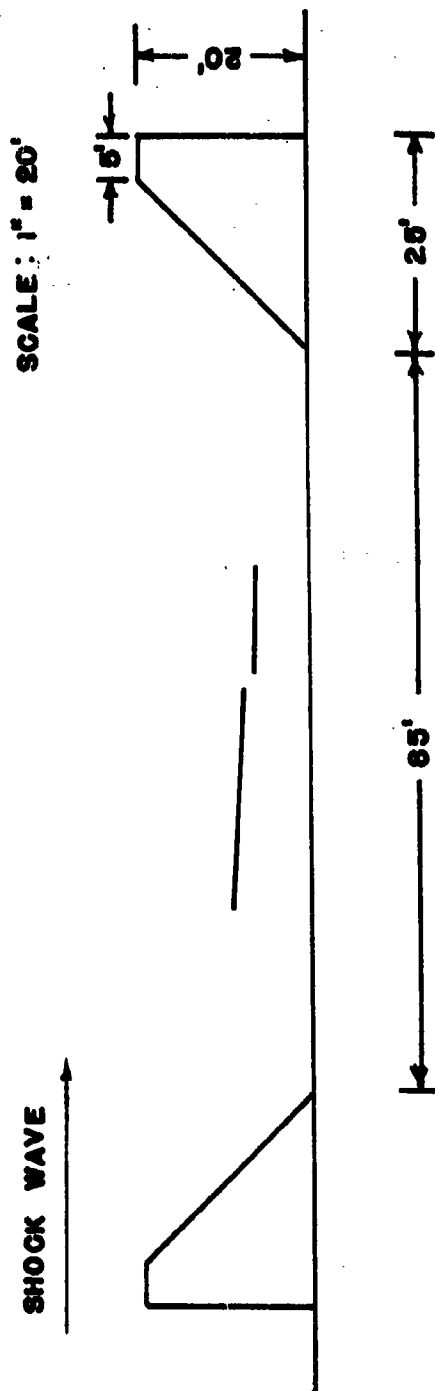


FIG. 7 PRESSURE-TIME RECORDS FROM CIRCULAR REVETMENT



**FIG. 8 FULL SIZE SLOPING REVEMENT FOR F-105D**



The assumption is made that static shock overpressure load will not crush the aircraft, but that the dynamic pressure from the air flow behind the shock wave may cause motion and perhaps damage. For ideal protection, no motion ought to occur.

Three forms of motion will be considered: translation along the longitudinal axis of the aircraft, vertical translation, and pitching about the lateral axis. Accordingly, drag force, lift force, and the pitching moment will be calculated. Translation should occur if

$$D_x > \mu W \quad (1)$$

where  $D_x$  is the total drag force in the horizontal direction,  $\mu$  is the static coefficient of wheel friction on concrete, and  $W$  is weight of aircraft. Vertical translation should occur if the flight condition

$$L_y > W \text{ is satisfied,} \quad (2)$$

where  $L_y$  is the lift force in the vertical direction. Pitching could occur if the aircraft lifts from the parked position; or, the nose wheel or tail may tend to break without the aircraft leaving the ground. The latter case involves strength of materials and stress analysis which is beyond the scope of the present study.

Table VI shows the values of  $L$ ,  $D$ , and  $M$ , the pitching moment about a moment center .35 of the mean aerodynamic chord. These values were computed from average velocity vectors and density at the wing and tail areas as shown above on Figure 8, for revetment Model II, at  $0^\circ$  Yaw. The coefficients of Reference 9 were used with values of dynamic pressure acting upon the control area,  $S$ , of  $385 \text{ ft}^2$  and for a mean aerodynamic chord,  $\bar{c}$ , of 11.485 ft. The forces and pitching moments were defined by the following three equations:

$$L = C_L (1/2 \rho u^2) S, \quad (3)$$

$$D = C_D (1/2 \rho u^2) S, \quad (4)$$

$$\text{and} \quad M = C_M (1/2 \rho u^2) S \bar{c} \text{ where} \quad (5)$$

$C_L$ ,  $C_D$ , and  $C_M$  are the coefficients for lift, drag, and pitching.  $\rho$  is the density and  $u$  is the magnitude of the flow velocity vector at the given point.  $D$  is defined to be parallel to the direction of  $u$  and  $L$  is defined to be perpendicular to the direction of  $u$ .

TABLE VI. VALUES OF LIFT, DRAG, AND PITCHING MOMENT  
MODEL II, YAW ANGLE 0°

WING PARAMETERS											
T,msec	$\alpha$ ,deg	$q$ ,lb/ft <sup>2</sup>	$C_L$	L,lb	$l_y$ ,lb	$C_D$	D,lb	$D_x$ ,lb	$C_M$	M,ft-lb	Remarks
29	-10.2	138	-.513	-27,142	-28,195	.150	7,931	-2,111	-.0815	-49,550	Specifications
38	- 5.3	206	-.224	-17,765	-18,423	.082	6,503	4,266	-.0615	-56,019	For F-105D:
48	- 4.2	174	-.179	-11,974	-12,460	.080	5,352	4,075	-.0590	-44,703	Weight 46,000lb
57	- 3.9	179	-.154	-10,613	-11,048	.073	5,031	3,977	-.0595	-47,076	Length 64' 3"
66	- 4.2	198	-.179	-13,668	-14,223	.080	6,122	4,664	-.0590	-51,690	Height 19' 8"
75	- 2.6	171	-.100	- 6,584	- 6,914	.069	4,546	4,025	-.0575	-43,479	Wing Span
84	- 1.2	178	-.036	- 2,467	- 2,690	.064	4,386	4,249	-.0585	-46,043	34' 11"
94	- 1.5	168	-.049	- 3,169	- 3,413	.067	4,312	4,120	-.0560	-41,564	Wing Area <sub>2</sub>
103	- 3.3	149	-.140	- 7,733	- 7,868	.071	4,073	3,799	-.0565	-37,227	385 ft
112	- 0.2	101	+.002	+ 78	+ 154	.063	2,450	2,449	-.0555	-24,788	$\bar{C}=11.485$ ft
121	0	97	+.015	+ 560	+ 636	.067	2,502	2,502	-.0555	-23,807	$\alpha=1.8^\circ$ for
149	- 2.6	74	-.098	- 281	- 437	.072	2,041	2,013	-.0575	-18,880	parked position

HORIZONTAL TAIL PARAMETERS											
29											Shock has not arrived at tail position.
38											
48	-3.0	145	-.026	-1,448	-1,451	.002	111	36	+.0407	+26,044	
57	-4.4	210	-.034	-2,749	-2,760	.002	243	30	+.0597	+55,435	
66	-3.0	189	-.026	-1,890	-1,890	.002	146	48	+.0407	+34,003	
75	-3.3	171	-.025	-1,646	-1,651	.002	132	37	+.0447	+33,800	
84	-0.1	218	-.008	- 671	- 671	.000	0	0	+.0014	+ 1,362	
94	+2.6	205	+.019	+1,497	+1,503	.002	157	90	-.0353	-31,969	
103	-1.7	113	-.013	- 566	- 566	.001	44	27	+.0231	+11,541	
112	-0.3	105	-.002	- 81	- 81	.000	0	0	+.0041	+ 1,906	
121	+1.2	96	+.009	+ 333	+ 334	.001	37	30	-.0163	- 6,919	
149	-3.0	86	-.026	- 864	- 865	.002	67	22	+.0407	+15,520	

It is seen from Table VI that the vertical lift force,  $L_y$ , is primarily negative (down). For the time it is positive it does not exceed the 46,000-pound gross weight of the aircraft. The aircraft should, therefore, not lift from the ground.

If a coefficient of static friction is assumed, for example, .25 for rubber on concrete with locked wheels, then it is seen that the horizontal drag force,  $D_x$ , is not great enough to equal one-quarter the weight of the airplane. No translation along the ground should occur. Since the aircraft does not leave the ground, no attempt will be made to interpret the pitching moments. Figures 9 - 11 show plots of vertical lift, horizontal drag, and pitching moment as functions of time for a yaw angle of  $0^\circ$  (shock wave approaching head-on). The steady free stream values for an unshielded aircraft are shown for comparison. The same procedure would be followed for angles other than  $0^\circ$  yaw.

A more elaborate application of the flow diagrams may be made by calculating the aerodynamic loading on several components of the aircraft for all the different flow vectors. The problem could then be coded for a machine solution.

For input data of aerodynamic loading and stress analysis, vulnerability and damage predictions could then be obtained for aircraft in revetments.

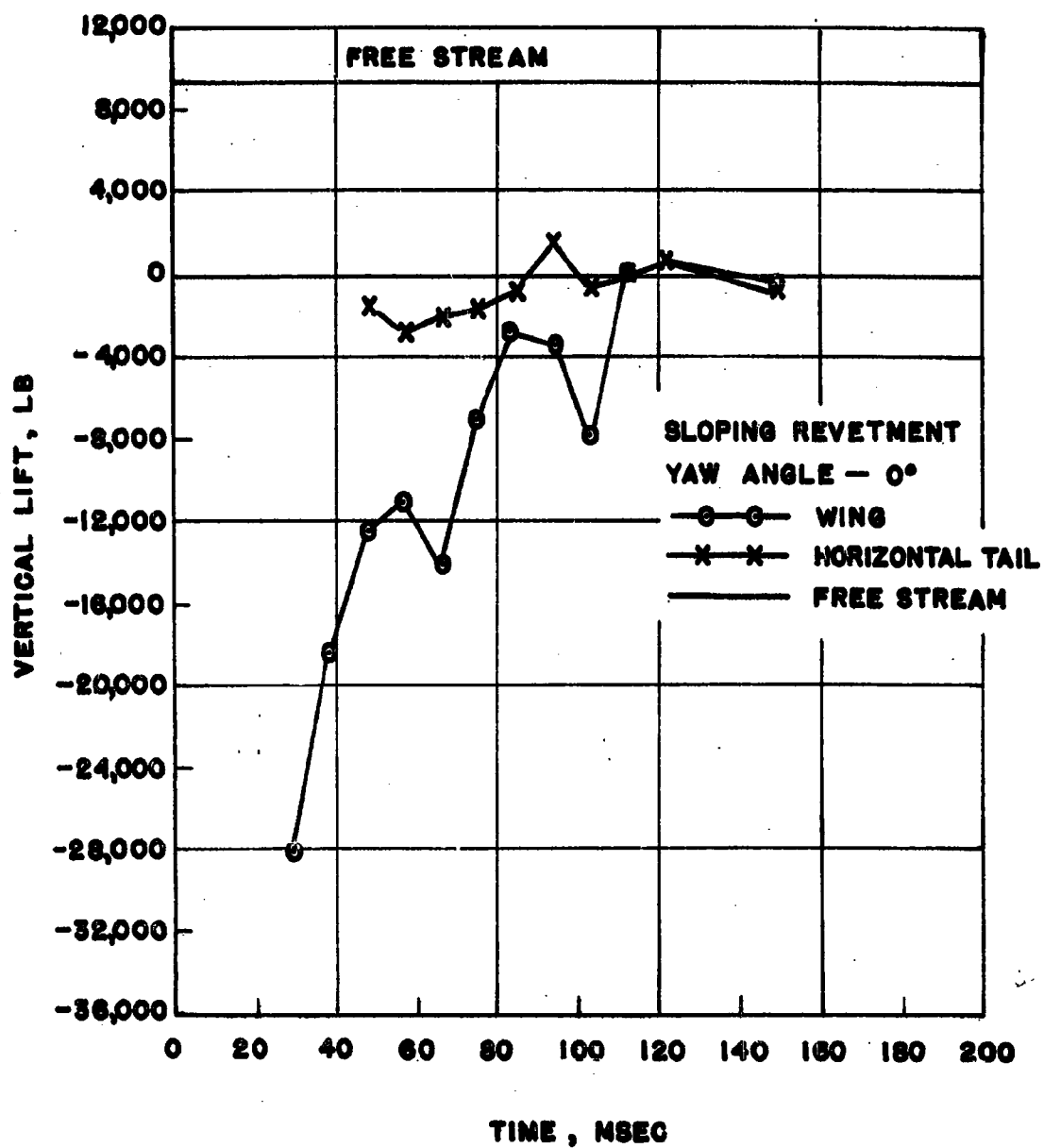


**FIG. 9 LIFT AS A FUNCTION OF TIME — YAW 0°  
SLOPING REVETMENT**

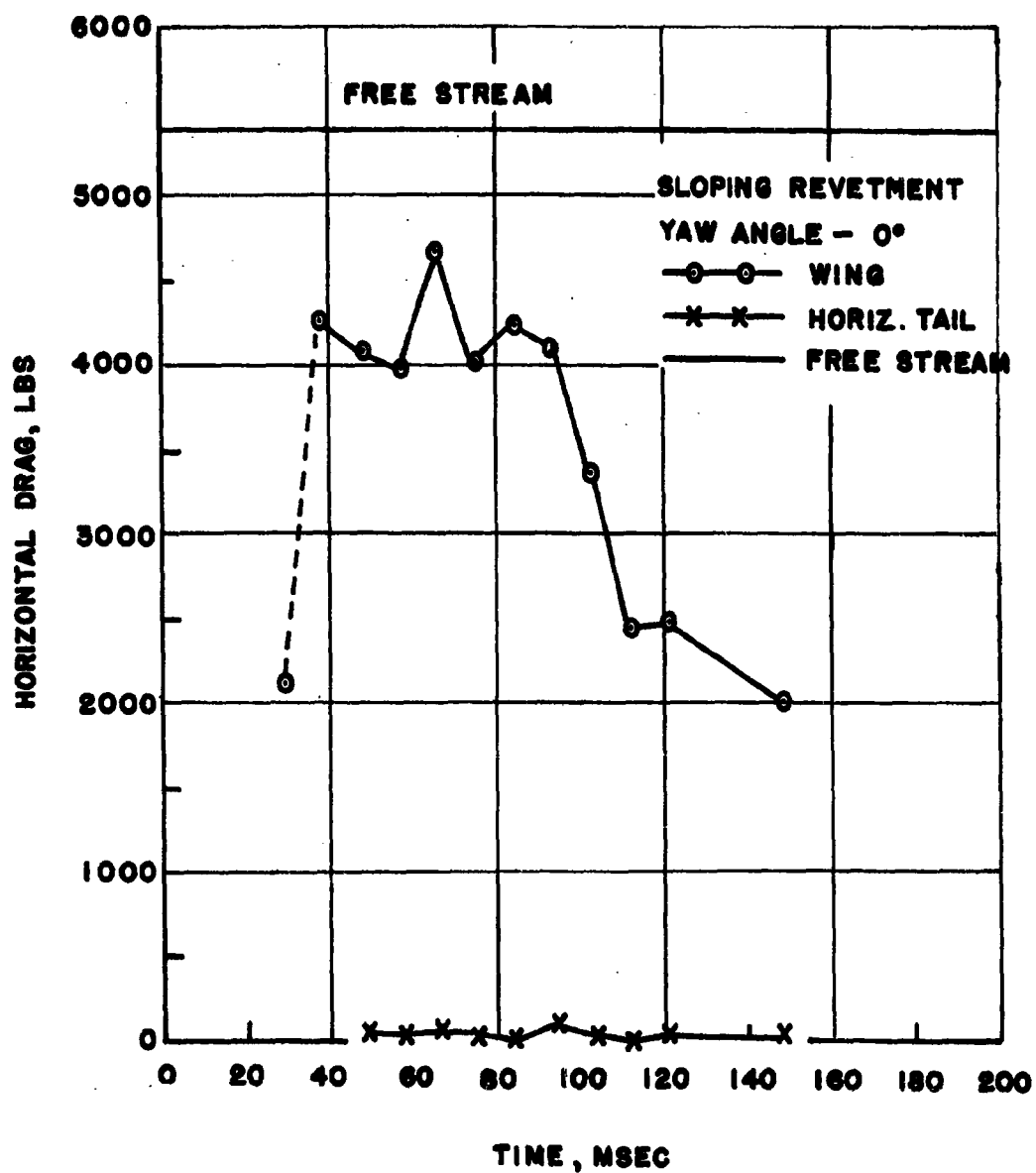


**FIG. 10 DRAG AS A FUNCTION OF TIME — YAW 0°  
 SLOPING REVETMENT**

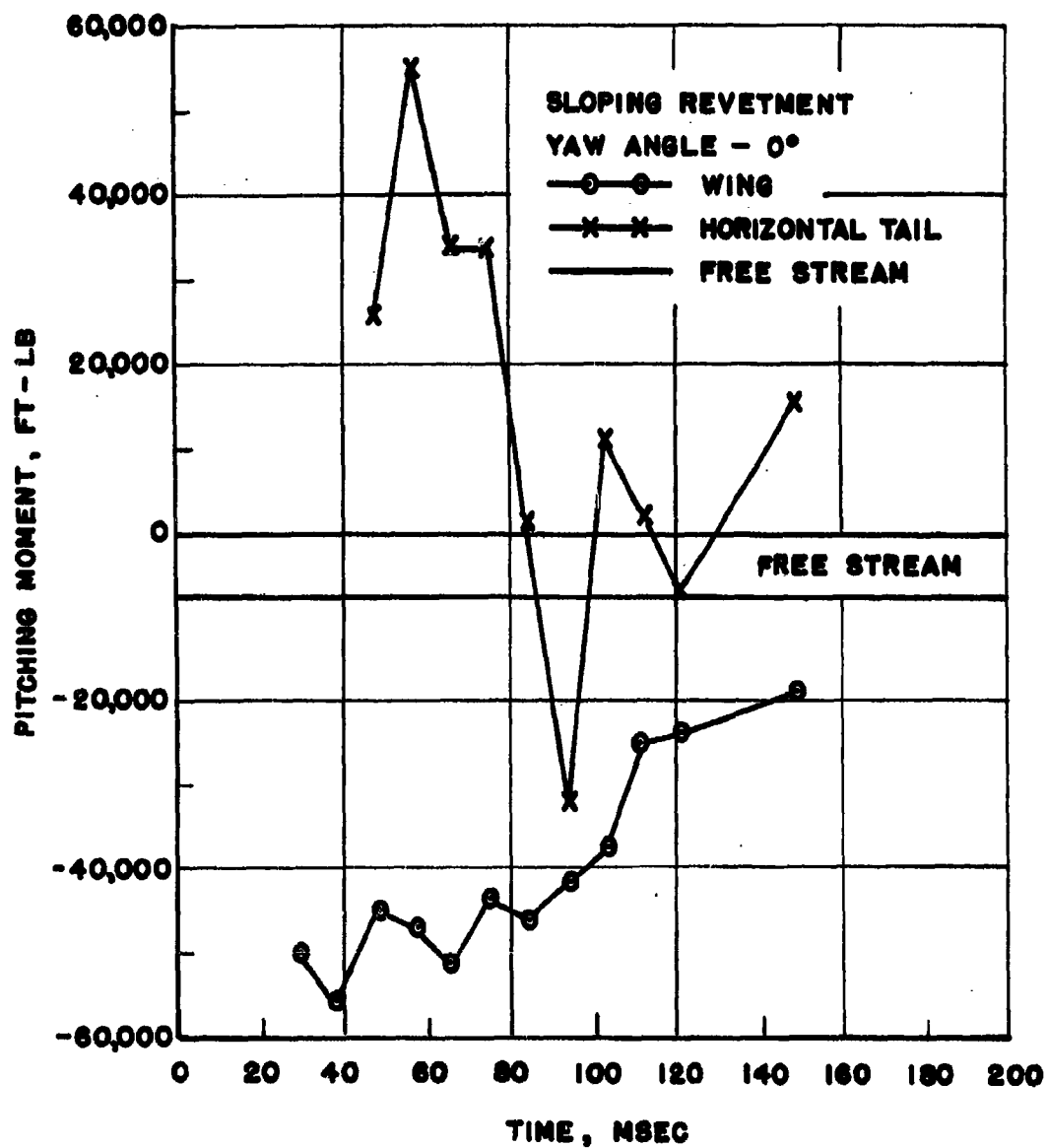


**FIG. 11 PITCHING MOMENT AS A FUNCTION OF TIME - YAW 0°;  
SLOPING REVETMENT**

## 5. DISCUSSION AND CONCLUSIONS

### 5.1 Discussion

The phenomena contributing to the flow patterns inside the model revetment were found to be the following: (1) diffraction of the input wave with vortex growth at the upstream part of the revetment, (2) reflection from the floor of the model after diffraction, (3) Mach stem growth of the shock wave after reflection, with travel across the floor of the model, (4) reflection of the Mach stem from the downstream portion of the model and the upstream travel of this reflection, and (5) an interaction of the reflection with the upstream vortex and the expansion of the reflection out of the model.

The vortex formation and steep flow angle were results of the shape of the upstream portion of the model. The straight inside edge caused the flow to be directed downward at a steep angle into the revetment. At about an inch from the model, the flow rotated upstream in the direction toward the model. In comparison, the  $45^\circ$  inside slope caused a downward flow at an angle of  $8^\circ$  at 200  $\mu\text{sec}$ . The angle changed to  $6^\circ$  for 548  $\mu\text{sec}$ . A less steep inside model slope would presumably cause still smaller angles of flow. A more nearly horizontal flow might be obtained in this way if desired.

The influence of the upward slope of the downstream portion of the revetment was seen for a distance of about one model height upstream, as seen by the upward direction of the flow. This was not true for the straight edge of Model III. A downward trend lasted throughout the entire observation period.

A flow magnitude greater than the free-stream value occurred at a time between 315 - 330  $\mu\text{sec}$ , for the Models I, II, and III. As was suggested in Reference 7, this was probably caused by the Mach reflection of the shock wave from the floor of the model. The flow directions were different as described above.

The changes in dimensions for Models I and II apparently were too small to cause a noticeable change in the flow patterns. The change in spacing between the two halves of the revetment did determine the arrival time of the return of the downstream reflection at the observation position; this determined how soon the flow speed decreased.

In general, the slope for the upstream portion of the revetment influenced the initial flow very strongly in both the direction and magnitude, had a slight effect upon the direction for intermediate times, but had little effect upon maximum speed, and in later times after the reflection had passed the observation position, affected only the direction of flow if the position were a distance within one model height away from the downstream sloping model.

Since the slope of the exterior wall of the model appeared not to influence the flow inside the model, a vertical outside wall should be used to offer protection against flying debris. A sloping outside wall may well deflect debris into the interior of the revetment to cause damage to the parked aircraft.

## 5.2 Conclusions

The inner wall should be designed with a slope which will direct the flow in an optimum direction for the particular aircraft to be protected. From this standpoint, the design of an optimum revetment must fit the lift and drag characteristics of the aircraft to be shielded.

Because of the strong vortex action at the upstream part of the revetment and also, the upward direction of flow for the downstream part of the model, the aircraft should probably be parked some distance away from the surrounding walls, a distance of one to two revetment heights, so that the effects of the vortex and the upward flow are a minimum at the aircraft position.

## ACKNOWLEDGEMENT

The authors wish to thank Mrs. Helen Malone for programming the data for machine computation.

*George A. Coulter*  
GEORGE A. COULTER

*Robert L. Peterson*  
ROBERT L. PETERSON



#### LIST OF REFERENCES

1. Coulter, George A. "Shielding Effect of Walls". Aberdeen Proving Ground, Maryland: BRL Technical Note No. 582, April, 1952.
2. "The Effects of Nuclear Weapons". Washington 25, D.C.; Department of the Army Pamphlet No. 39-3, May 1, 1957.
3. Bryant, E. J. and Day, J. D. "Effects of Rough Terrain on Drag - Sensitive Targets". AFSWP Sandia Base, Albuquerque, New Mexico: Operation Plumbbob, Project 1.8b, ITR 1408, December, 1957.
4. Hoerner, Sigward F. "Fluid-Dynamic Drag". 148 Busted Drive, Midland Park, New Jersey: Published by the author, 1958.
5. Coulter, George A. and Matthews, William T. "Changes in Drag Caused by Air Blast Shielding". Aberdeen Proving Ground, Maryland: BRL Memorandum Report No. 1279, DASA 1157, June, 1960.
6. Muirhead, J. C., Lecuyer, D. W., and McCallum, F. L., "A Method for the Observation of Air Movement in Shock Tube Flows Using Smoke Streams as Tracers". Suffield Experimental Station, Canada: Suffield Technical Paper No. 153, January 9, 1959.
7. Teel, George D. "A Study of Flow Patterns in Aircraft Revetments". Aberdeen Proving Ground, Maryland: BRL Memorandum Report, To be published.
8. Clark, Robert O. "Preliminary Shock Tube Study of Aircraft Revetment Design". Aberdeen Proving Ground, Maryland: BRL Technical Note No. 983, AFSWP No. 776, January, 1955.
9. Moore, K. "F-105 Airplane - Investigation of Landing - Gear Effects on the 1/4-Scale Model in the WADC 20-Foot Wind Tunnel". Farmingdale, New York: Republic Aviation Corporation EAR-400, December 19, 1957.
10. Cancro, Patrick A. and Kelly, H. Neale. "Investigation of a 1/4-Scale Model of the Republic F-105 Airplane in the Langley 19-Foot Pressure Tunnel - Longitudinal Stability and Control and Horizontal-Tail Hinge - Moment and Normal - Force Characteristics of the Model Equipped with a Drooped Supersonic - Type Elliptical Wing - Root Inlet". NACA RM SL55KO7, November 30, 1955.

APPENDIX A

TABLES FOR COMPARISON OF FLOW

APPENDIX A  
TABLES FOR COMPARISON OF FLOW

TABLE A-I. COMPARISON OF FLOW VECTORS - MODEL I

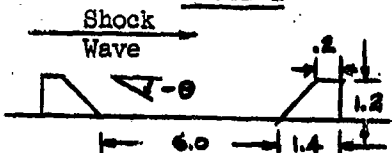
Time, μsec	Position, in.		Flow Speed, ft/sec	Angle, deg	Density Ratio, $\rho/\rho_1$	Remarks
200	2.20	.34	314	-8.4	1.27	<p style="text-align: center;">Model I</p> 
	2.27	.66	343	-5.6	1.26	
	2.39	.37	325	-6.2		
240	2.40	.35	348	-5.8		<p style="text-align: center;">Free Stream Shock Parameters</p>
	2.60	.66	358	-5.9		
	2.70	.68	402	-5.3		
316	2.75	.34	353	-7.9	1.28	<p> <math>P_s = 8.3</math> psi  <math>u_2 = 375</math> ft/sec  <math>U = 1379</math> ft/sec  <math>\rho_1 = .00231</math> slugs/ft<sup>3</sup>  <math>\rho_2 = .00316</math> slugs/ft<sup>3</sup> </p>
	2.73	.65	354	-7.8	1.29	
	3.00	.35	380	-4.7		
	3.00	.67	405	-8.1		
355	2.85	.32	358	-3.7	1.30	<p>Mach reflection is about 3/4 the height of the model.</p>
	3.05	.64	372	-7.8		
	3.16	.34	313	-4.2		
	3.17	.65	383	-7.7		
	3.65	.75	356	-3.9		
432	3.21	.33	342	-7.7		<p>Reflection starts from downstream model.</p>
	3.43	.34	326	-5.0		
	3.43	.67	357	-4.8		
	3.78	.65	362	-1.2		
548	3.67	.32	330	-4.0		
	4.00	.34	281	-2.5		
	4.00	.66	305	-6.4		
	4.28	.63	335	-4.1		
625	3.96	.32	261	0.0		<p>Reflection has passed smoke position.</p>
	4.15	.34	292	0.0		
	4.20	.66	271	+2.5		
	4.59	.64	199	-7.2		
702	4.10	.32	205	-9.8		
	4.40	.33	164	-8.4		
	4.40	.66	196	-5.6		
	4.69	.65	211	+1.1		
856	4.65	.33	297	0.0		<p>Vortex interaction with reflection.</p>
	4.90	.37	303	+1.1		
	5.17	.65	295	-9.4		

TABLE A-I. (CONTINUED) COMPARISON OF FLOW VECTORS - MODEL I

Time, $\mu$ sec	Position, in.		Flow Speed, ft/sec	Angle, deg	Density Ratio, $\rho/\rho_1$	Remarks
x	y					
932	3.21	.17	279	-9.5		
	3.75	.41	248	-16.2		
	4.60	.31	244	-10.8		
1088	3.70	.24	184	-6.8		Reflection is out of model.
	4.25	.35	201	-14.4		
	5.05	.58	185	-14.7		

TABLE A-II. COMPARISON OF FLOW VECTORS - MODEL II

Time, μsec	Position, in.		Flow Speed, ft/sec	Angle, deg	Density Ratio, $\rho/\rho_1$	Remarks
	x	y				
121	.90	.31	307	- 7.1		<p>Shock Model II</p> <p>Wave</p> <p>Free Stream Shock</p> <p>Parameters</p> <p><math>P_2 = 8.3</math> psi</p> <p><math>u_2 = 375</math> ft/sec</p> <p><math>U = 1380</math> ft/sec</p> <p><math>\rho_1 = .00231</math> slugs/ft<sup>3</sup></p> <p><math>\rho_2 = .00316</math> slugs/ft<sup>3</sup></p> <p>Mach reflection from shock wave.</p>
	.92	.55	319	-11.5		
	.94	.79	328	-14.2		
	1.10	.33	302	- 8.6	1.25	
	1.11	.56	308	-12.1	1.21	
	1.13	.84	318	-14.9	1.21	
160	1.06	.30	313	- 5.6		
	1.08	.53	336	- 7.9		
	1.12	.77	353	- 5.8		
	1.26	.32	334	- 1.7	1.33	
	1.29	.55	343	- 6.2	1.31	
	1.30	.80	352	-12.1	1.33	
198	1.19	.28	291	- 6.9		
	1.23	.51	341	- 5.5		
	1.26	.76	304	- 9.0		
	1.41	.32	319	- 4.4	1.37	
	1.43	.53	304	- 5.4	1.43	
	1.44	.77	321	- 7.0	1.39	
	2.36	.38	354	- 3.8	1.51	
	2.35	.60	330	- 6.7	1.38	
	2.36	.85	301	- 7.5	1.31	
	2.54	.38	287	- 3.1	1.52	
	2.54	.62	276	- 7.1	1.38	
	2.55	.86	362	- 6.2	1.31	
237	1.33	.27	329	- 3.3		<p>Mach stem is near middle smoke stream.</p>
	1.36	.50	318	- 7.0		
	1.40	.73	363	- 7.9		
	1.56	.30	339	- 2.6	1.43	
	1.57	.52	324	- 4.4	1.51	
	1.60	.76	348	- 5.6	1.42	
	2.53	.36	341	- 5.1	1.45	
	2.53	.59	351	- 3.8	1.48	
	2.51	.84	341	- 3.0	1.34	
	2.72	.37	365	- 3.6	1.47	
	2.72	.60	353	- 4.7	1.48	
	2.72	.85	341	- 3.9	1.34	

TABLE A-II. (CONTINUED) COMPARISON OF FLOW VECTORS - MODEL II

Time, $\mu\text{sec}$	Position, in.		Flow Speed, ft/sec	Angle, deg	Density Ratio, $\rho/\rho_1$	Remarks
x	y					
275	1.49	.27	305	- 2.0		
	1.52	.47	303	- 6.2		
	1.56	.71	318	- 8.1		
	1.72	.30	315	- 4.4	1.35	Mach stem arrived at downstream model. Mach stem is higher than smoke grid.
	1.73	.51	335	- 5.2	1.53	
	1.76	.74	314	- 3.5	1.23	
	2.67	.35	306	- 3.2	1.41	
	2.68	.58	323	- 3.1	1.44	
	2.68	.83	365	- 3.1	1.43	
	3.45	.38	350	- 3.6	1.18	
	3.45	.62	351	- 3.9	1.21	
	3.45	.88	355	- 5.4	1.24	
	3.64	.39	319	- 2.7	1.18	
	3.64	.63	351	- 3.5	1.21	
	3.63	.88	343	- 3.3	1.24	
314	1.61	.26	309	- 3.6		
	1.64	.47	308	- 2.9		
	1.69	.69	320	- 8.9		
	1.85	.28	313	- 6.9	1.45	Mach stem reflects from downstream model. Reflection travels back upstream.
	1.87	.49	324	- 5.8	1.48	
	1.89	.75	322	+ 1.1	1.35	
	2.82	.34	325	- 3.2	1.38	
	2.83	.57	325	- 5.4	1.49	
	2.85	.82	337	- 4.5	1.32	
	3.04	.34	328	- 3.4	1.38	
	3.04	.58	318	- 3.6	1.49	
	3.02	.82	342	- 4.6	1.32	
	3.61	.38	347	+ 0.9	1.33	
	3.61	.61	357	+ 0.7	1.24	
	3.62	.85	385	- 2.5	1.20	
	3.80	.38	356	+ 0.3	1.33	
352	1.78	.25	321	- 1.9		
	1.80	.46	331	- 3.7		
	1.85	.67	338	- 6.9		
	2.01	.27	340	- 2.2	1.35	Reflection continues upstream.
	2.03	.48	329	- 3.0	1.41	
	2.06	.74	355	- 9.5	1.27	
	2.98	.34	359	- 1.5	1.54	
	2.98	.55	370	- 1.2	1.34	
	2.99	.81	336	- 3.6	1.38	
	3.18	.34	340	+ 1.2	1.54	
	3.17	.57	342	- 1.9	1.34	

TABLE A-II. (CONTINUED) COMPARISON OF FLOW VECTORS - MODEL II

Time, $\mu$ sec	Position, in.		Flow Speed, ft/sec	Angle, deg	Density Ratio, $\rho/\rho_1$	Remarks
391	3.18	.82	374	- 2.4	1.38	Reflection continues.
	3.78	.39	283	+ 5.7	1.50	
	3.78	.61	307	+ 7.1		
	3.81	.86	315	+ 6.6		
	3.95	.39	268	+10.4	1.50	
	3.94	.65	302	+11.5		
	3.95	.89	322	+ 6.9		
	1.91	.25	286	- 1.6		
	1.94	.45	305	- 4.6		
	2.00	.65	317	- 6.5		
	2.16	.26	300	+ 2.0	1.41	
	2.18	.48	316	- 1.9	1.44	
	2.21	.69	320	-10.2	1.44	
	3.15	.33	327	+ 1.3	1.69	
	3.17	.56	333	+ 2.9	1.68	
	3.16	.80	332	- 0.2	1.48	
	3.36	.35	300	+ 2.7	1.69	
	3.36	.57	327	+ 2.9	1.68	
	3.37	.81	322	+ 3.1	1.48	
	3.88	.41	207	+ 9.1	1.39	
	3.90	.65	227	+13.7	1.44	
	4.06	.43	222	+19.9	1.39	
429	2.04	.24	302	- 5.3		Reflection continues.
	2.08	.43	298	- 6.3		
	2.14	.63	318	- 2.9		
	2.28	.28	285	- 0.5	1.40	
	2.32	.47	298	- 3.9	1.45	
	2.35	.69	307	- 5.3	1.36	
	2.89	.28	250	- 1.7	1.57	
	3.28	.34	242	+ 5.8	1.65	
	3.29	.57	245	+ 5.5	1.59	
	3.30	.81	285	+ 7.7	1.61	
	3.46	.36	214	+ 5.2	1.65	
	3.47	.58	232	+ 7.7	1.59	
	3.48	.83	246	+12.2	1.61	
	3.97	.42	176	+15.8		
	3.99	.67	217	+19.3	1.43	
	4.02	.94	258	+24.9	1.43	
	4.15	.46	195	+27.7		
	4.19	.71	227	+23.5	1.43	
	4.22	.98	272	+29.9	1.43	

TABLE A-II. (CONTINUED) COMPARISON OF FLOW VECTORS - MODEL II

Time, $\mu\text{sec}$	Position, in. x y		Flow Speed, ft/sec	Angle, deg	Density Ratio, $\rho/\rho_1$	Remarks
468	2.19	.22	250	- 4.5		
	2.21	.41	246	- 2.0	1.45	
	2.29	.64	263	- 4.7		
	2.42	.26	246	- 1.4	1.45	
	2.45	.46	239	- 0.3	1.59	
	2.50	.67	253	- 4.3	1.44	
	3.38	.36	202	+ 2.5	1.60	
	3.40	.58	255	+ 7.2	1.62	
	3.42	.83	247	+10.5	1.47	
	3.55	.37	188	+ 3.4	1.60	
	3.57	.60	214	+ 9.0	1.60	
	3.59	.86	251	+13.1	1.47	
	4.04	.45	198	+22.7	1.28	
	4.09	.72	249	+23.9	1.26	
	4.22	.51	191	+26.6	1.28	
	4.28	.77	259	+27.1	1.26	
						Reflection has passed smoke grid position.
506	2.27	.22	220	- 1.2		
	2.30	.42	236	- 1.8	1.50	
	2.38	.61	224	- 8.3		
	2.51	.27	233	+ 1.2	1.53	
	2.54	.47	223	+ 0.8	1.58	
	2.58	.67	220	- 3.8	1.45	
	3.47	.35	219	- 0.1	1.63	
	3.49	.60	221	+ 5.4	1.56	
	3.53	.85	205	+10.1	1.67	
						Reflection continues upstream.
545	2.39	.22	194	- 1.8		
	2.43	.41	200	- 4.3		
	2.50	.61	207	- 2.7		
	2.64	.27	217	- 4.4	1.49	
	2.66	.46	216	- 5.9	1.59	
	2.70	.65	218	- 0.9	1.47	
	3.58	.35	220	+ 2.6	1.54	
	3.60	.60	229	+ 6.9	1.53	
	3.62	.87	263	+10.4	1.41	
583	2.45	.22	160	- 2.5	1.42	
	2.51	.40	175	- 3.0		
	2.58	.60	176	- 5.9		
	2.71	.26	164	- 1.8	1.42	
	2.74	.45	184	- 3.2	1.55	
	2.79	.67	200	- 3.0	1.45	



TABLE A-II. (CONTINUED) COMPARISON OF FLOW VECTORS - MODEL II

Time, $\mu\text{sec}$	Position, in. x y		Flow Speed, ft/sec	Angle, deg	Density Ratio, $\rho/\rho_1$	Remarks
622	3.67	.36	208	+15.3		Reflection begins to interact with vortex from upstream model. Flow speed be- comes less at this time.
	3.72	.62	230	+16.5	1.38	
	3.77	.90	267	+13.6	1.42	
	3.86	.42	205	+12.2		
	3.90	.65	231	+16.9	1.38	
	3.99	.94	269	+18.0	1.42	
	2.54	.21	211	- 3.1		Reflection is caught in the vortex.
	2.60	.40	207	- 4.4	1.50	
	2.66	.59	221	- 7.2		
	2.79	.26	230	- 1.8	1.49	
	2.83	.45	226	0.0	1.41	
	2.88	.64	226	- 8.1	1.42	
	3.77	.41	216	+13.1	1.59	
	3.81	.66	270	+14.5	1.33	
	3.95	.44	240	+14.3	1.59	
	4.01	.71	278	+17.9	1.33	
660	2.64	.21	254	- 3.4		
	2.70	.39	247	- 2.7		
	2.78	.58	249	- 1.3		
	2.92	.25	254	- 3.3	1.47	
	2.95	.45	254	- 3.5	1.38	
	3.00	.64	251	- 3.3	1.38	
	3.87	.41	234	+ 7.0		
	3.97	.69	274	+11.8	1.34	
	3.99	.95	282	+11.7		
	4.07	.47	238	+16.9		
	4.15	.73	290	+18.5	1.34	
	4.20	1.03	345	+16.6		
699	2.77	.20	244	- 0.7		
	2.82	.39	263	- 1.6		
	2.89	.58	265	- 2.0		
	3.02	.25	239	- 3.2	1.49	
	3.06	.44	277	- 2.1	1.51	
	3.11	.63	290	- 0.3	1.39	
737	2.87	.21	254	- 0.7		
	2.94	.38	273	- 4.8		
	3.02	.57	297	- 3.9		
	3.14	.24	264	- 3.1		

TABLE A-II. (CONTINUED) COMPARISON OF FLOW VECTORS - MODEL II

Time, $\mu\text{sec}$	Position, in. x y		Flow Speed, ft/sec	Angle, deg	Density Ratio, $\rho/\rho_1$	Remarks
	3.20	.44	274	- 2.3		
	3.26	.64	312	- 3.7		
776	3.01	.20	281	- 3.1		
	3.08	.37	276	- 1.7		
	3.16	.57	292	+ 1.6		
	3.27	.24	274	+ 1.6	1.38	Reflection is out of view.
	3.31	.43	254	- 0.4	1.51	
	3.40	.60	269	+ 0.4	1.42	
814	3.13	.20	237	- 2.8		
	3.20	.37	234	- 0.3		
	3.29	.58	252	- 3.6		
	3.40	.24	259	- 0.1	1.47	
	3.44	.44	242	+ 3.1	1.47	
	3.51	.64	267	+13.9	1.40	
853	3.22	.19	194	- 1.7		
	3.29	.37	200	- 0.9		
	3.40	.55	225	+ 2.1		
	3.51	.24	200	- 2.8	1.45	
	3.54	.44	203	+ 0.9	1.39	
	3.64	.66	236	+13.4	1.31	
891	3.31	.19	272	+ 0.4		Flow now has a positive direction for this position. Vortex appears to be breaking up, less defined.
	3.38	.37	201	+ 4.0		
	3.50	.58	219	+ 8.3		
	3.58	.24	175	+10.4		
	3.63	.44	254	+ 8.4		
	3.72	.69	231	+12.4		
930	3.42	.19	210	+ 0.2		
	3.47	.38	221	+ 4.7		
	3.59	.58	223	+ 8.2		
	3.66	.27	204	+ 9.4		
	3.74	.47	234	+12.1		
	3.84	.71	234	+ 3.5		
968	3.50	.19	173	+ 7.7		
	3.58	.39	214	+ 3.0		
	3.77	.27	215	+10.1		

TABLE A-III. COMPARISON OF FLOW VECTORS - MODEL III

Time, $\mu$ sec	Position, in.		Flow Speed, ft/sec	Angle, deg	Remarks
x	y				
160	2.40	.78	29	-52	Shock Wave
	2.40	1.10	118	-42	
183	2.60	.34	52	-62	Model III
	2.60	1.10	71	-70	
205	3.00	.90	27	-63	Note: Data taken from Teel, Ref. 7.
	3.00	1.12	44	-36	
222	2.45	.32	448	-1	Free Stream Shock Parameters
	2.50	.75	320	-18	
	2.50	.95	359	-24	
	3.10	1.10	350	-21	
244	2.60	.32	48	-11	$P_2 = 8.0$ psi $u_2 = 365$ ft/sec $U = 1375$ ft/sec $\rho_1 = .00231$ slugs/ft <sup>3</sup> $\rho_2 = .00314$ slugs/ft <sup>3</sup>
	2.60	.75	117	-36	
	2.60	.95	187	-51	
267	2.50	.95	395	-24	Note: Density measurements not available.
	3.05	.35	287	-7	
	3.05	.77	310	-6	
	3.08	1.10	350	-21	
284	2.95	.32	327	-6	
	3.00	.70	371	-14	
	3.00	.90	378	-16	
	3.55	.75	329	-13	
307	2.90	.35	348	-10	
	2.90	.75	375	-13	
	2.90	.95	386	-17	
329	3.30	.34	389	-5	
	3.40	.77	371	-9	
	3.50	1.10	403	-19	
346	2.95	.32	327	-6	
	3.00	.70	371	-14	
	3.00	.90	378	-16	
	3.55	.75	329	-13	
369	3.25	.30	345	-6	
	3.00	.90	378	-16	
	3.55	.75	329	-13	

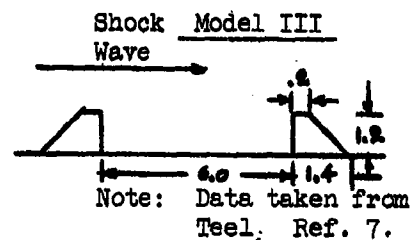


TABLE A-II. (CONTINUED) COMPARISON OF FLOW VECTORS - MODEL II

Time, μsec	Position, in.		Flow Speed, ft/sec	Angle, deg	Density Ratio, $\rho/\rho_1$	Remarks
x	y					
1007	3.58	.21	236	+ 7.0		
	3.67	.39	218	+ 4.6		
	3.81	.62	236	+ 4.3		
	3.86	.30	231	+10.9		
	3.95	.51	241	+12.4		
	3.82	.62	297	+18.5		
1046	3.79	.40	249	+ 7.0		Vortex is broken up.
1084	3.82	.20	173	+ 1.3		
	3.90	.42	233	+13.3		
	4.06	.63	249	+13.1		
	4.07	.33	211	+16.1		
	4.15	.54	260	+21.6		
	4.31	.79	218	+ 4.0		
1122	3.88	.22	152	- 8.9		
	4.00	.45	111	- 0.6		
	4.23	.73	161	+11.9		Flow becomes erratic.
1161	3.93	.22	173	+12.0		
	4.00	.42	126	- 2.3		
	4.22	.37	119	+ 6.1		
	4.34	.63	124	+11.9		

TABLE A-III. (CONTINUED) COMPARISON OF FLOW VECTORS - MODEL III

Time, μsec	Position, in.		Flow Speed, ft/sec	Angle, deg	Remarks
x	y				
391	3.55	.32	299	- 7	
	3.55	.75	329	-13	
408	3.10	.33	307	- 7	
	3.25	.70	303	-15	
431	3.40	.30	379	- 9	
	3.40	.72	392	-10	
	3.30	.90	388	-20	
453	3.82	.75	360	-10	
470	3.42	.30	319	- 9	
	3.50	.70	336	-12	
	3.50	.90	364	-17	
493	3.50	.30	292	-10	
	3.55	.70	354	- 6	
	3.60	.90	407	-16	
515	4.05	.32	333	- 6	
	3.50	.70	336	-12	
532	3.56	.30	404	- 5	
	3.57	.55	397	-17	
	3.60	.75	359	-19	
554	3.90	.30	284	- 3	
	3.92	.60	316	-12	
	3.70	.75	330	-21	
594	3.90	.30	78	-24	
	3.90	.55	143	-10	
	3.70	.75	169	- 8	
617	4.00	.30	263	- 7	
	4.02	.62	260	- 5	

TABLE A-IV. COMPARISON OF FLOW VECTORS - MODEL V

Time, μsec	Position, in.		Flow Speed, ft/sec	Angle, deg	Density, <sup>3</sup> slugs/ft	q, lb/ft <sup>2</sup>	Remarks
x	y						
72	.710	.412	158.2	-55.1	.00246	30.8	
	.736	.634	230.5	-53.3	.00247	65.6	
	.761	.858	286.5	-44.4	.00258	105.9	
	.994	.671	195.3	-34.4	.00247	47.1	
	1.014	.911	119.6	-28.7	.00258	18.4	
110	.731	.382	176.6	-41.7	.00262	40.9	Free Stream Shock Parameters P <sub>2</sub> = 8.6 psi u <sub>2</sub> = 385 ft/sec U = 1392 ft/sec ρ <sub>1</sub> = .00231 slugs/ft <sup>3</sup> ρ <sub>2</sub> = .00319 slugs/ft <sup>3</sup> P <sub>1</sub> = 14.7 psi
	.767	.591	236.0	-52.9	.00258	71.7	
	.808	.812	296.4	-48.1	.00262	114.9	
	1.031	.646	218.8	-48.3	.00258	61.6	
	1.062	.884	250.9	-44.4	.00262	32.4	

Model V

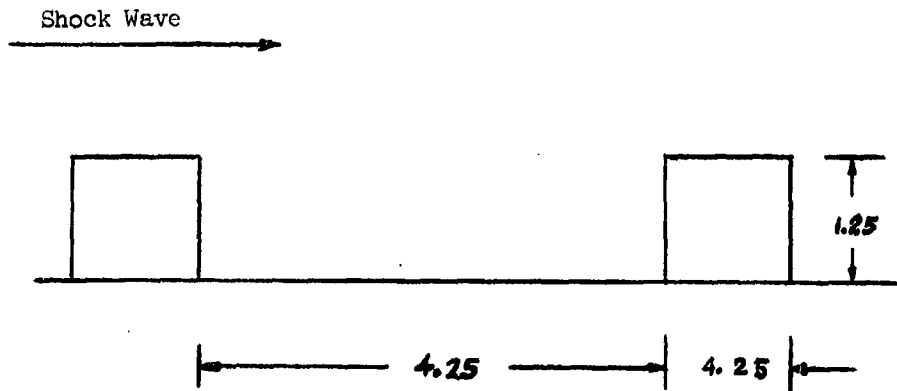


(Table A-IV continued on next page)

TABLE A-IV. (CONTINUED) COMPARISON OF FLOW VECTORS - MODEL V

Time, μsec	Position, in.		Flow Speed, Angle,		Density, <sup>3</sup>	q,	Remarks
	x	y	ft/sec	deg	slugs/ft <sup>3</sup>	lb/ft <sup>2</sup>	
148	.787	.146	143.5	-40.2	.00322	33.1	
	.798	.322	181.0	-46.9	.00320	52.4	
	.834	.503	233.4	-44.3	.00292	79.6	
	.902	.707	297.9	-53.3	.00283	125.6	Shock
	1.042	.154	163.7	-18.1	.00322	43.2	wave
	1.069	.360	207.8	-34.2	.00320	69.1	is
	1.105	.562	245.6	-39.2	.00292	88.1	about
	1.148	.799	306.1	-42.7	.00283	132.5	midway
	1.731	.199	138.3	-15.0	.00264	25.3	across
	1.751	.450	193.6	-33.2	.00256	47.9	model.
	1.763	.675	221.0	-38.2	.00277	67.5	
	1.787	.908	244.4	-31.4	.00283	84.2	
	1.977	.210	102.4	-24.0	.00204	13.8	
	1.988	.479	146.1	-38.1	.00256	27.3	
	2.004	.698	154.5	-32.2	.00277	33.0	
187	.834	.107	131.0	-10.6	.00372	32.0	
	.850	.266	159.4	-21.3	.00324	41.2	
	.908	.430	201.6	-35.1	.00296	60.1	
	.982	.600	263.5	-24.4	.00316	109.7	
	1.125	.127	185.4	-11.3	.00372	64.0	
	1.154	.302	219.2	- 8.4	.00324	77.8	
	1.194	.490	250.6	-18.2	.00296	92.9	
	1.266	.691	307.7	-19.8	.00316	149.5	
	1.317	.172	212.4	- 7.5	.00335	75.6	
	1.342	.378	239.9	-20.2	.00299	86.0	
	1.370	.583	264.8	-26.2	.00303	106.3	
	1.399	.821	301.6	-33.5	.00266	121.1	
	1.549	.185	208.4	- 6.6	.00335	72.7	
	1.552	.414	235.0	- 9.0	.00299	82.5	
	1.594	.642	253.8	-28.1	.00303	97.7	
	1.607	.887	294.8	-30.0	.00266	115.7	
	1.832	.172	253.7	+ 1.6	.00344	110.7	
	1.850	.385	257.1	- 1.8	.00316	104.4	
	1.865	.595	271.6	- 9.5	.00286	105.7	
	1.903	.837	283.0	-19.5	.00281	112.4	
	2.058	.194	244.3	+ 0.8	.00344	102.7	
	2.080	.407	263.2	- 0.8	.00316	109.3	
	2.101	.637	267.8	-11.2	.00286	102.7	
	2.123	.874	276.2	-24.8	.00281	107.1	

TABLE A-IV. (CONTINUED) COMPARISON OF FLOW VECTORS - MODEL V

Time, μsec	Position, in. x y		Flow Speed, Angle ft/sec deg		Density, <sup>3</sup> slugs/ft <sup>3</sup>	q, lb/ft <sup>2</sup>	Remarks
225	.892	.096	134.3	-17.9	.00390	35.1	
	.915	.241	146.9	-46.1	.00310	33.5	
	.975	.383	181.7	-53.6	.00305	50.4	
	1.081	.555	235.7	-42.3	.00298	82.7	
	1.206	.110	183.3	-13.4	.00390	65.4	
	1.251	.288	210.5	-31.0	.00310	68.8	
	1.304	.454	242.4	-28.3	.00305	89.6	
	1.382	.649	262.3	-29.3	.00298	102.4	
	1.413	.159	244.4	- 6.3	.00305	109.1	
	1.431	.346	236.9	- 9.1	.00305	85.5	
	1.473	.532	255.8	-17.9	.00331	108.2	
	1.516	.744	298.0	-20.1	.00288	128.1	
	1.643	.174	236.7	- 7.4	.00365	102.3	
	1.666	.396	276.5	-11.7	.00305	116.4	
	1.703	.584	278.9	-15.3	.00331	128.6	
	1.735	.812	305.1	-13.9	.00288	134.2	
	1.960	.175	279.7	-10.5	.00344	110.7	
	1.968	.382	293.9	-13.7	.00316	104.4	
	1.984	.575	302.9	-12.6	.00286	105.7	
	2.020	.796	202.0	-14.4	.00281	112.4	
	2.194	.175	297.6	- 5.3	.00344	102.7	
	2.205	.405	289.6	-10.3	.00316	109.3	
	2.230	.611	291.7	-16.0	.00286	102.7	
	2.241	.819	297.8	-12.3	.00281	107.1	
	2.301	.212	258.6	0.0	.00315	105.3	
	2.307	.467	242.4	- 7.6	.00276	84.3	
	2.321	.671	266.2	-13.7	.00276	97.6	
	2.332	.910	261.9	-21.4	.00259	89.0	
	2.522	.233	200.8	- 3.9	.00315	63.5	
	2.537	.487	214.6	- 5.2	.00287	66.1	
	2.546	.698	226.6	-17.2	.00276	70.8	
	2.551	.934	263.8	-16.6	.00259	90.3	
263	.953	.076	90.5	-29.1	.00459	18.8	
	.960	.194	102.9	-10.6	.00344	18.2	
	1.025	.315	154.5	-30.7	.00301	35.9	
	1.161	.483	196.2	-66.6	.00293	56.3	
	1.289	.090	164.0	- 4.8	.00459	61.7	
	1.333	.239	175.0	- 9.5	.00344	52.6	
	1.398	.403	217.5	-18.1	.00301	71.1	
	1.485	.591	264.1	-24.0	.00293	102.1	
	1.543	.145	224.4	-13.4	.00413	104.1	
	1.556	.326	245.8	-14.3	.00313	94.5	
	1.590	.494	257.8	-12.5	.00330	109.8	
	1.645	.697	282.5	-16.6	.00284	113.4	



TABLE A-IV. (CONTINUED) COMPARISON OF FLOW VECTORS - MODEL V

Time, μsec	Position, in.		Flow Speed, Angle, ft/sec deg		Density slugs/ft <sup>3</sup>	q, lb/ft <sup>2</sup>	Remarks
	x	y					
	1.768	.157	259.3	- 1.8	.00413	139.0	
	1.806	.367	274.1	-12.9	.00313	117.6	
	1.835	.548	276.4	-13.0	.00330	126.1	
	1.867	.780	295.7	-18.9	.00284	124.3	
	2.087	.152	285.7	+ 3.1	.00346	141.2	
	2.116	.345	297.8	+ 1.7	.00333	147.8	
	2.138	.541	311.8	- 6.4	.00336	163.1	
	2.168	.758	312.4	- 4.6	.00324	158.2	
	2.331	.163	289.8	+ 1.6	.00346	145.2	
	2.344	.380	299.7	- 3.9	.00333	149.8	
	2.362	.573	305.3	- 5.1	.00336	156.4	
	2.382	.789	317.7	- 7.7	.00324	163.6	
	2.444	.212	290.1	- 6.5	.00312	131.2	
	2.455	.447	294.6	-10.0	.00327	141.9	
	2.462	.637	310.4	- 7.2	.00340	163.6	
	2.466	.858	315.7	- 9.7	.00278	138.5	
	2.656	.226	303.4	- 3.5	.00312	143.6	
	2.656	.476	292.7	-10.9	.00327	140.0	
	2.674	.659	293.6	- 9.0	.00340	146.4	
	2.685	.894	296.8	-12.2	.00278	122.4	
	2.832	.183	295.2	- 3.5	.00304	132.5	
	2.836	.449	236.7	- 5.4	.00294	120.9	
	2.839	.646	294.6	- 4.6	.00327	141.9	
	2.861	.877	291.6	-11.2	.00265	112.5	
	3.055	.192	256.1	- 3.0	.00304	99.7	
	3.069	.470	271.7	-10.6	.00294	108.6	
	3.074	.673	261.8	-11.0	.00327	112.1	
	3.093	.904	279.8	-15.4	.00265	103.6	
302	.969	.067	44.6	-76.0	.00438	4.35	
	.989	.188	92.6	-76.9	.00309	13.3	Shock
	1.074	.286	129.4	-64.2	.00330	27.6	wave
	1.190	.416	174.2	-50.0	.00307	46.5	has
	1.355	.085	147.8	- 1.5	.00438	47.8	reflected
	1.398	.228	170.3	-26.1	.00309	44.8	from
	1.487	.374	215.4	-32.3	.00330	76.5	downstream
	1.599	.541	254.6	-22.3	.00307	99.4	part
	1.619	.127	195.8	- 9.0	.00368	70.6	of
	1.655	.300	234.0	-13.6	.00308	84.4	model.
	1.704	.469	287.7	-14.5	.00326	134.8	
	1.766	.660	292.3	-19.6	.00299	127.8	
	1.883	.154	270.7	- 6.1	.00308	135.0	
	1.916	.342	259.3	- 9.7	.00308	103.7	
	1.952	.521	276.8	-12.9	.00326	124.9	

TABLE A-IV. (CONTINUED) COMPARISON OF FLOW VECTORS - MODEL V

Time, μsec	Position, in.		Flow Speed, ft/sec	Angle, deg	Density, <sup>3</sup> slugs/ft <sup>3</sup>	q, lb/ft <sup>2</sup>	Remarks
x	y						
	1.999	.735	309.5	-16.2	.00299	143.3	
	2.221	.159	285.0	-13.1	.00342	139.0	
	2.237	.349	280.6	- 7.6	.00340	134.0	
	2.266	.526	288.6	-10.7	.00336	140.0	
	2.302	.747	312.0	-13.7	.00308	149.7	
	2.460	.166	299.4	- 4.2	.00342	153.3	
	2.478	.371	302.2	- 6.5	.00340	155.4	
	2.505	.561	320.1	- 6.2	.00336	172.3	
	2.528	.769	323.7	- 8.3	.00308	161.2	
	2.511	.197	317.4	- 2.5	.00315	158.6	
	2.518	.425	307.3	- 4.5	.00309	146.1	
	2.605	.619	313.0	- 7.0	.00313	153.4	
	2.614	.832	337.7	- 7.6	.00301	171.6	
	2.804	.217	326.4	- 8.0	.00315	167.3	
	2.806	.447	341.2	- 4.4	.00309	180.1	
	2.812	.637	324.4	- 3.8	.00313	164.8	
	2.819	.865	321.7	-12.2	.00301	155.7	
302	2.980	.174	328.5	- 0.7	.00335	180.7	
	2.988	.434	323.7	- 4.9	.00321	168.4	
	2.997	.633	335.7	- 6.7	.00344	193.8	
	3.008	.848	326.8	- 7.4	.00293	156.7	
	3.192	.184	324.6	+ 0.6	.00335	176.3	
	3.214	.443	321.3	- 1.4	.00321	165.8	
	3.214	.646	358.1	- 3.7	.00344	188.8	
	3.237	.864	328.1	- 8.7	.00293	158.0	
	3.393	.210	324.5	-13.4	.00315	166.0	
	3.395	.459	325.0	- 4.5	.00316	166.8	
	3.402	.662	314.9	- 3.3	.00302	149.7	
	3.418	.888	321.3	- 7.9	.00305	157.3	
	3.599	.215	305.5	- 7.5	.00316	147.1	
	3.595	.468	315.6	- 7.0	.00315	157.3	
	3.603	.675	295.7	- 8.1	.00302	132.1	
	3.626	.901	293.0	- 9.7	.00305	130.3	
340	.975	.045	41.1	-159.4	.00448	3.78	
	1.002	.134	78.7	-77.5	.00370	11.5	
	1.101	.230	108.3	-104.0	.00314	18.4	
	1.246	.349	167.8	-93.1	.00279	39.3	
	1.425	.083	154.5	-20.7	.00448	53.4	
	1.479	.188	172.6	-21.8	.00370	55.2	
	1.575	.318	210.4	-11.8	.00314	69.5	
	1.700	.499	217.0	-38.5	.00279	65.7	
	1.722	.110	215.0	+ 3.2	.00376	86.8	
	1.768	.273	238.9	- 5.8	.00298	85.2	

TABLE A-IV. (CONTINUED) COMPARISON OF FLOW VECTORS - MODEL V

Time, μsec	Position, in. x y		Flow Speed, ft/sec	Angle, deg	Density, <sup>3</sup> slugs/ft	q, lb/ft <sup>2</sup>	Remarks
	1.851	.431	266.2	- 7.5	.00358	126.7	
	1.903	.612	281.8	-12.5	.00326	129.4	
	2.019	.139	255.2	- 3.1	.00376	122.3	
	2.043	.320	268.3	- 4.3	.00298	107.4	
	2.086	.490	285.5	- 4.0	.00358	145.8	
	2.142	.693	302.2	- 6.3	.00326	148.8	
	2.346	.130	271.1	- 0.9	.00364	133.9	
	2.376	.331	281.9	-11.1	.00318	125.7	
	2.400	.501	296.9	- 7.6	.00329	144.8	
	2.451	.711	321.9	-13.9	.00313	162.1	
	2.606	.156	295.8	- 4.1	.00364	159.4	
	2.621	.354	302.9	- 6.9	.00318	146.0	
	2.655	.544	311.9	-10.0	.00329	159.8	
	2.677	.747	337.3	-11.1	.00313	178.0	
	2.739	.190	316.6	+ 0.8	.00347	173.9	
	2.739	.413	319.2	- 3.8	.00314	160.1	
	2.752	.601	314.5	- 5.7	.00301	149.0	
	2.777	.811	331.9	- 4.3	.00312	171.9	
	2.958	.195	316.3	+ 3.0	.00347	173.6	
	2.971	.434	319.2	- 1.5	.00314	163.7	
	2.974	.626	329.0	- 5.1	.00301	163.1	
	2.978	.830	326.1	- 0.7	.00312	165.9	
	3.138	.172	359.6	- 2.9	.00326	211.0	
	3.136	.421	350.3	- 1.8	.00323	198.3	
	3.150	.615	330.1	- 5.4	.00344	187.5	
	3.161	.828	338.3	- 5.8	.00295	168.6	
	3.357	.186	320.9	- 4.6	.00326	168.1	
	3.366	.439	307.2	- 3.9	.00323	152.6	
	3.380	.635	313.1	- 1.7	.00344	168.7	
	3.391	.841	314.9	- 3.8	.00295	146.1	
	3.545	.174	255.8	+14.0	.00359	117.4	
	3.554	.447	266.9	- 4.7	.00289	103.1	
	3.559	.653	268.7	-12.4	.00301	108.8	
	3.574	.866	277.8	- 5.1	.00333	128.4	
	3.764	.194	211.8	-10.0	.00359	80.5	
	3.758	.449	219.1	+18.4	.00289	69.4	
	3.754	.653	221.2	+ 2.0	.00301	73.7	
	3.764	.877	233.6	+13.4	.00333	90.8	
378	.960	.040	71.5	-142.3	.00503	12.8	
	1.006	.118	87.0	-143.1	.00337	12.7	
	1.092	.194	121.6	-140.9	.00287	21.2	
	1.242	.282	167.9	+65.6	.00323	45.6	
	1.492	.058	105.9	-24.8	.00503	28.2	

TABLE A-IV. (CONTINUED) COMPARISON OF FLOW VECTORS - MODEL V

Time, μsec	Position, in.		Flow Speed, ft/sec	Angle, deg	Density, slugs/ft <sup>3</sup>	q, lb/ft <sup>2</sup>	Remarks
	x	y					
	1.543	.163	141.2	-31.8	.00337	33.6	
	1.562	.300	190.4	-37.3	.00287	52.0	
	1.771	.443	211.4	-27.9	.00323	72.3	
	1.615	.117	228.8	- 8.9	.00367	95.9	
	1.574	.252	239.4	-14.5	.00309	88.5	
	1.947	.418	246.8	-18.2	.00328	99.8	
	2.017	.587	280.6	-18.2	.00316	124.5	
	2.120	.134	268.6	- 4.9	.00357	132.2	
	2.104	.311	267.4	-15.6	.00309	110.4	
	2.215	.481	297.1	-17.8	.00328	144.6	
	2.274	.678	309.7	-15.5	.00316	151.7	
	2.467	.128	249.9	- 2.9	.00366	114.1	
	2.492	.307	258.4	- 3.6	.00332	110.8	
	2.536	.483	262.0	- 8.0	.00324	111.2	
	2.590	.676	276.5	- 5.6	.00325	124.1	
	2.731	.146	204.9	- 1.6	.00366	76.7	
	2.754	.338	217.6	- 4.8	.00332	78.6	
	2.789	.521	222.5	- 1.5	.00324	80.2	
	2.834	.716	253.4	+ 5.7	.00325	104.2	
	2.867	.192	268.6	- 5.9	.00321	115.6	
	2.875	.403	297.9	- 5.1	.00321	142.6	
	2.897	.586	314.2	- 6.3	.00317	156.3	
	2.923	.800	312.4	- 7.8	.00306	149.2	
	3.097	.203	233.9	-14.7	.00321	87.7	
	3.117	.431	243.6	- 5.0	.00321	95.4	
	3.111	.613	253.7	- 8.1	.00317	110.1	
	3.119	.825	277.8	-19.6	.00306	117.9	
	3.319	.133	203.9	-58.0	.00422	57.2	
	3.313	.416	209.3	+ 5.7	.00397	87.4	
	3.300	.600	213.4	+11.3	.00407	92.7	
	3.320	.812	258.2	+20.6	.00379	96.9	
	3.450	.175	161.8	-63.7	.00422	55.3	
	3.499	.430	170.2	+42.0	.00397	57.4	
	3.505	.691	164.3	+26.6	.00407	53.1	
	3.573	.852	215.2	+43.8	.00339	78.4	
	3.624	.194	99.4	+59.0	.00425	21.0	
	3.642	.439	125.9	+63.4	.00385	33.5	
	3.750	.623	159.8	+53.8	.00414	52.8	
	3.775	.837	178.1	+49.5	.00383	60.8	
	3.824	.187	66.8	+33.3	.00425	9.5	
	3.833	.401	72.6	+58.4	.00385	10.2	
	3.897	.635	115.4	+62.6	.00414	27.6	
	3.839	.835	154.2	+62.0	.00383	45.6	

TABLE A-IV. (CONTINUED) COMPARISON OF FLOW VECTORS - MODEL V

Time, μsec	Position, in. x y		Flow Speed, ft/sec	Angle, deg	Density, slugs/ft <sup>3</sup>	q lb/ft <sup>2</sup>	Remarks
417	.921	.009	97.9	-180.0	.00752	36.1	
	.955	.080	100.4	-176.4	.00354	17.8	
	1.034	.146	139.7	-140.4	.00275	26.8	
	1.206	.203	160.5	-147.3	.00323	41.6	
	1.516	.047	82.5	- 12.5	.00752	25.6	
	1.595	.130	127.8	- 24.9	.00354	29.0	
	1.731	.248	167.5	- 15.5	.00275	38.5	
	1.863	.394	226.0	- 19.4	.00323	82.5	
	1.934	.098	224.9	- 3.4	.00381	96.3	
	1.987	.233	225.5	- 12.2	.00317	80.6	
	2.073	.376	245.7	- 15.4	.00343	103.6	
	2.155	.541	265.2	- 20.7	.00304	107.0	
	2.269	.121	262.6	+ 1.1	.00381	131.3	
	2.287	.277	241.9	- 2.1	.00317	92.7	
	2.356	.436	260.4	- 5.5	.00343	116.4	
	2.424	.637	268.4	- 12.2	.00304	109.6	
	2.575	.123	144.4	- 13.0	.00441	46.0	
	2.608	.300	146.3	+ 29.1	.00415	44.4	
	2.639	.468	154.5	+ 25.3	.00396	47.2	
	2.700	.666	168.9	+ 26.6	.00380	54.2	
	2.794	.145	97.5	+ 15.9	.00441	21.0	
	2.819	.333	113.6	+ 33.7	.00415	26.8	
	2.857	.519	129.3	+ 25.6	.00396	33.1	
	2.906	.723	130.2	+ 22.6	.00380	32.2	
	2.989	.179	160.5	+ 24.8	.00446	57.4	
	3.016	.391	188.5	+ 64.8	.00403	71.6	
	3.043	.570	194.0	+ 49.4	.00412	77.6	
	3.067	.780	199.4	+ 30.1	.00384	76.3	
	3.173	.183	115.6	+ 60.3	.00446	29.8	
	3.197	.418	135.1	+ 42.9	.00403	36.8	
	3.219	.599	163.5	+ 49.4	.00412	55.1	
	3.235	.807	193.7	+ 46.2	.00384	72.0	
	3.306	.177	55.7	+ 27.9	.00379	5.88	
	3.331	.418	58.6	+ 26.6	.00404	6.93	
	3.348	.609	143.2	+ 49.4	.00431	31.7	
	3.378	.834	142.2	+ 35.0	.00340	32.1	
	3.489	.192	46.5	+ 19.7	.00379	4.09	
	3.518	.447	63.4	+ 51.3	.00404	8.12	
	3.530	.644	106.0	+ 48.1	.00431	24.3	
	3.574	.875	158.6	+ 51.9	.00340	42.7	
	3.630	.203	48.0	+ 32.0	.00394	4.53	
	3.655	.465	87.5	+ 54.7	.00381	14.6	
	3.680	.680	132.2	+ 51.6	.00376	32.9	
	3.716	.906	178.8	+ 54.3	.00400	63.9	

TABLE A-IV. (CONTINUED) COMPARISON OF FLOW VECTORS - MODEL V

Time, $\mu$ sec	Position, in. x y		Flow Speed, Angle, ft/sec deg		Density, <sup>3</sup> slugs/ft <sup>3</sup>	q, lb/ft <sup>2</sup>	Remarks
	3.798	.219	58.5	+22.6	.00394	6.74	
	3.811	.485	89.1	+51.6	.00381	15.1	
	3.832	.704	151.1	+62.4	.00376	43.0	
	3.870	.953	194.8	+55.8	.00400	75.9	
455	2.026	.092	140.1	- 5.4	.00384	37.7	Mach reflection formed from downstream and reflection is about in middle of the model.
	2.079	.213	135.2	-13.2	.00339	31.0	
	2.166	.351	148.0	- 9.9	.00363	39.8	
	2.251	.505	166.3	- 2.0	.00338	46.7	
	2.365	.123	118.0	-39.8	.00384	26.8	
	2.385	.273	143.9	+ 5.7	.00339	35.1	
	2.450	.427	132.7	+ 7.1	.00363	32.0	
	2.510	.617	154.2	+ 8.4	.00338	40.2	
	2.599	.118	50.2	- 9.5	.00450	5.66	
	2.624	.309	60.7	-29.1	.00371	6.85	
	2.673	.485	82.8	-31.4	.00374	12.8	
	2.740	.685	89.9	-31.4	.00368	14.9	
	2.819	.152	68.4	- 8.5	.00450	10.5	
	2.852	.354	79.9	-18.4	.00371	11.8	
	2.903	.541	95.1	-14.0	.00374	16.9	
	2.950	.741	101.3	+11.3	.00368	18.9	
	3.012	.190	66.1	+30.5	.00403	8.79	
	3.031	.422	70.0	-10.0	.00386	9.46	
	3.065	.595	94.2	+15.4	.00382	16.9	
	3.101	.800	110.4	+23.6	.00370	22.6	
	3.188	.208	82.9	+19.8	.00403	13.8	
	3.222	.441	84.0	+29.7	.00386	13.6	
	3.251	.637	114.4	+26.6	.00382	25.0	
	3.278	.852	150.8	+30.7	.00370	42.1	
	3.337	.194	55.3	+12.5	.00368	5.61	
	3.364	.434	77.9	+36.9	.00408	12.4	
	3.391	.660	124.6	+28.4	.00388	30.2	
	3.433	.872	151.2	+39.1	.00345	39.4	
	3.514	.201	60.7	+37.6	.00368	6.78	
	3.539	.474	95.1	+47.7	.00408	18.4	
	3.577	.696	133.6	+50.4	.00388	34.7	
	3.626	.942	177.8	+44.1	.00345	54.5	
	3.659	.221	66.9	+45.0	.00376	8.40	
	3.686	.508	117.6	+47.6	.00346	23.9	
	3.722	.732	143.0	+55.0	.00346	35.4	
	3.776	.989	204.8	+47.5	.00373	78.2	
	3.820	.228	61.0	+67.6	.00376	6.99	
	3.845	.528	122.9	+66.6	.00346	26.2	
	3.872	.779	174.6	+63.4	.00346	52.8	
	3.935	1.049	243.5	+56.3	.00373	110.6	

TABLE A-IV. (CONTINUED) COMPARISON OF FLOW VECTORS - MODEL V

Time, μsec	Position, in.		Flow Speed, ft/sec	Angle, deg	Density, <sup>3</sup> slugs/ft	q, lb/ft <sup>2</sup>	Remarks
x	y						
493	2.064	.089	60.1	-114.0	.00449	8.09	*
	2.110	.206	45.7	- 80.5	.00344	3.60	
	2.207	.344	62.7	- 26.6	.00378	7.43	
	2.303	.503	77.0	- 43.8	.00361	10.7	
	2.376	.114	42.2	- 21.0	.00449	3.99	
	2.421	.277	59.6	- 41.2	.00344	6.12	
	2.479	.431	62.0	- 34.7	.00378	7.27	
	2.566	.624	76.4	- 24.4	.00361	10.5	
	2.621	.114	69.2	- 2.5	.00441	10.6	
	2.657	.291	95.7	+ 4.1	.00381	17.5	
	2.706	.465	90.8	- 4.6	.00376	15.5	
	2.772	.666	112.5	+ 4.8	.00349	22.1	
	2.856	.146	93.4	- 8.4	.00441	19.2	
	2.885	.344	96.8	+ 7.6	.00381	17.9	
	2.939	.532	113.5	+ 14.0	.00376	24.2	
	2.995	.751	130.4	+ 17.1	.00349	29.7	
	3.043	.208	65.7	- 45.0	.00364	7.87	
	3.061	.416	82.6	+ 18.4	.00382	13.0	
	3.117	.610	91.6	+ 20.6	.00367	15.4	
	3.159	.825	122.6	+ 22.9	.00351	26.3	
	3.233	.224	80.7	0.0	.00364	11.9	
	3.260	.463	82.6	+ 22.4	.00382	13.0	
	3.302	.662	106.0	+ 31.0	.00367	20.7	
	3.345	.892	137.5	+ 30.3	.00351	33.1	
	3.353	.197	63.6	+ 12.3	.00342	6.91	
	3.393	.456	104.9	+ 28.1	.00370	20.3	
	3.434	.684	121.0	+ 31.0	.00397	29.0	
	3.490	.919	165.2	+ 34.8	.00340	46.4	
	3.537	.219	71.2	+ 32.9	.00342	8.65	
	3.575	.514	117.7	+ 24.9	.00370	25.6	
	3.612	.738	149.2	+ 38.1	.00397	44.2	
	3.684	.998	206.2	+ 41.7	.00340	72.3	
	3.679	.241	76.4	+ 22.2	.00356	10.4	
	3.724	.550	102.5	+ 33.7	.00350	18.4	
	3.760	.787	160.6	+ 49.4	.00355	45.8	
	3.836	1.054	225.9	+ 50.4	.00379	96.8	
	3.832	.259	74.5	+ 36.9	.00356	9.89	
	3.868	.582	128.1	+ 57.3	.00350	28.7	
	3.906	.848	188.1	+ 57.8	.00355	62.8	
	3.997	1.141	261.8	+ 56.1	.00379	130.0	

TABLE A-IV. (CONTINUED) COMPARISON OF FLOW VECTORS - MODEL V

Time, $\mu$ sec	Position, in. x y		Flow Speed, ft/sec	Angle, deg	Density, <sup>3</sup> slugs/ft <sup>3</sup>	q, lb/ft <sup>2</sup>	Remarks
532	2.057	.072	36.5	-26.6	.00467	3.11	
	2.111	.195	63.2	-10.9	.00319	6.38	Mach
	2.222	.337	57.2	-43.0	.00366	5.99	stem
	2.316	.489	73.1	-39.0	.00344	9.18	reflection
	2.399	.105	62.5	+ 9.5	.00467	9.11	has
	2.435	.264	64.4	-12.8	.00319	6.63	interacted
	2.502	.414	81.2	+ 2.2	.00366	12.1	with
	2.585	.615	76.7	-10.5	.00344	10.1	vortex.
	2.662	.112	98.4	- 2.1	.00445	21.5	
	2.707	.295	100.5	+ 2.5	.00355	17.9	
	2.751	.461	112.5	+ 5.4	.00362	22.9	
	2.838	.671	128.6	+ 7.9	.00333	27.6	
	2.904	.139	103.8	+11.3	.00445	24.0	
	2.939	.351	117.8	+11.7	.00355	24.1	
	3.004	.548	126.2	+ 4.2	.00362	28.8	
	3.065	.772	149.1	- 1.6	.00333	37.0	
	3.061	.190	99.3	+ 1.5	.00356	17.5	
	3.105	.431	111.2	0.0	.00355	22.0	
	3.146	.621	118.1	+10.5	.00367	25.6	
	3.206	.845	153.2	+22.0	.00347	40.7	
	3.260	.224	88.5	+11.3	.00356	13.9	
	3.291	.476	112.1	+24.0	.00355	22.3	
	3.338	.684	146.2	+22.6	.00367	39.3	
	3.389	.917	149.5	+29.2	.00347	38.8	
	3.395	.206	104.4	+34.2	.00326	17.8	
	3.447	.485	123.7	+32.6	.00375	28.7	
	3.489	.716	142.2	+42.9	.00366	37.0	
	3.556	.964	195.8	+37.9	.00307	58.9	
	3.568	.239	68.5	+36.9	.00326	7.65	
	3.626	.537	126.8	+54.5	.00375	30.2	
	3.679	.790	177.0	+57.0	.00366	57.3	
	3.767	1.072	216.2	+49.9	.00307	71.7	
	3.718	.257	86.0	+47.0	.00361	13.4	
	3.756	.571	108.4	+52.1	.00349	20.5	
	3.814	.850	181.2	+53.6	.00329	54.0	
	3.914	1.148	293.7	+49.8	.00379	163.5	
	3.861	.280	70.5	+42.5	.00301	8.96	
	3.401	.633	123.4	+55.8	.00349	26.5	
	3.959	.931	212.6	+60.6	.00329	74.3	
	4.071	1.251	402.7	+38.3	.00379	307.4	



TABLE A-IV. (CONTINUED) COMPARISON OF FLOW VECTORS - MODEL V

Time, $\mu$ sec	Position, in. x y		Flow Speed, Angle, ft/sec deg		Density, <sup>3</sup> slugs/ft <sup>3</sup>	q, lb/ft <sup>2</sup>	Remarks
570	2.072	.065	41.4	-14.0	.00452	3.87	
	2.158	.186	71.7	-73.3	.00346	8.88	
	2.249	.311	74.8	+90.0	.00372	10.4	
	2.354	.458	124.3	0.0	.00368	28.4	
	2.432	.110	82.3	-24.4	.00346	15.3	
	2.475	.255	82.0	-24.0	.00452	11.6	
	2.549	.416	102.8	-15.1	.00372	19.6	
	2.634	.606	133.0	- 2.8	.00368	32.6	
	2.711	.110	127.9	0.0	.00440	36.0	
	2.749	.297	124.0	- 1.4	.00348	26.7	
	2.809	.467	149.7	- 1.3	.00370	41.5	
	2.890	.678	161.7	+ 2.2	.00335	43.9	
	2.950	.148	117.0	0.0	.00440	30.1	
	2.991	.362	142.9	- 2.7	.00348	35.5	
	3.053	.552	149.9	+ 4.7	.00370	41.6	
	3.129	.770	194.8	+14.5	.00355	63.5	
	3.128	.192	112.6	+25.3	.00366	23.2	
	3.163	.431	113.7	+19.8	.00354	22.9	
	3.224	.635	136.1	+24.6	.00357	33.1	
	3.291	.879	167.2	+16.4	.00330	46.2	
	3.315	.235	100.9	+10.8	.00366	18.6	
	3.356	.505	127.1	+ 4.4	.00354	28.6	
	3.425	.720	151.3	+27.6	.00357	40.9	
	3.467	.961	171.2	+29.2	.00330	48.4	
	3.440	.237	107.8	+18.4	.00337	19.6	
	3.492	.514	109.2	+19.8	.00397	23.7	
	3.539	.763	143.8	+23.0	.00370	38.3	
	3.637	1.027	200.2	+40.6	.00351	70.3	
	3.590	.255	83.8	+16.5	.00337	11.8	
	3.662	.588	134.8	+31.0	.00397	36.0	
	3.722	.857	174.6	+31.6	.00370	56.4	
	3.825	1.141	272.8	+40.5	.00351	130.5	
608	2.093	.060	55.6	-10.6	.00493	7.62	
	2.164	.168	60.2	-29.1	.00328	5.94	
	2.249	.279	99.2	+ 3.5	.00355	17.5	
	2.421	.458	128.6	- 7.9	.00332	27.4	
	2.471	.092	105.2	+ 1.9	.00493	27.3	
	2.508	.241	88.8	- 4.4	.00328	12.9	
	2.596	.403	113.2	- 9.2	.00355	22.8	
	2.708	.602	165.9	- 7.8	.00332	45.6	
	2.780	.110	133.4	-13.6	.00462	41.1	
	2.821	.295	152.1	-20.4	.00358	41.4	
	2.888	.465	188.9	+ 2.2	.00355	63.3	

TABLE A-IV. (CONTINUED) COMPARISON OF FLOW VECTORS - MODEL V

Time, μsec	Position, in. x y		Flow Speed, ft/sec	Angle, deg	Density, slugs/ft <sup>3</sup>	q lb/ft <sup>2</sup>	Remarks
	2.986	.682	210.8	+ 4.2	.00316	70.2	
	3.011	.148	141.6	- 1.5	.00462	46.4	Small
	3.069	.358	148.1	- 7.1	.00358	39.2	portion
	3.141	.559	181.4	+ 4.0	.00355	58.4	of
	3.241	.799	216.6	+ 3.7	.00316	74.1	Mach
	3.163	.208	124.8	- 6.6	.00361	28.1	stem
	3.208	.447	139.6	+14.0	.00352	34.3	has
	3.268	.655	155.8	+15.1	.00332	40.3	reflected
	3.353	.897	192.8	+20.1	.00342	63.7	from
	3.353	.242	107.5	0.0	.00361	20.9	upstream
	3.403	.508	155.6	+19.4	.00352	42.6	wall.
	3.467	.742	139.4	+16.5	.00332	32.3	
	3.528	.995	223.2	+24.9	.00342	85.3	
	3.483	.251	95.3	+14.6	.00313	14.2	
	3.537	.530	142.1	+35.4	.00371	37.5	
	3.599	.789	174.6	+39.0	.00353	53.8	
	3.700	1.081	222.4	+37.9	.00267	66.1	
	3.639	.269	115.7	+37.2	.00313	21.0	
	3.716	.620	127.8	+35.8	.00371	30.3	
	3.792	.901	197.9	+50.1	.00353	69.1	
	3.950	1.248	256.0	+45.0	.00267	87.6	
646	2.122	.054	61.0	+ 7.6	.00466	8.67	
	2.196	.150	57.5	- 6.3	.00338	5.60	
	2.309	.282	94.4	-45.0	.00340	15.2	
	2.473	.451	102.1	-46.7	.00330	17.2	
	2.526	.094	72.0	+ 8.1	.00466	12.1	
	2.555	.237	110.8	0.0	.00338	20.8	
	2.652	.394	120.0	- 9.5	.00340	24.5	
	2.788	.592	153.2	+10.0	.00330	38.7	
	2.832	.098	141.5	+ 4.1	.00451	45.2	
	2.885	.271	149.8	+11.9	.00371	41.6	
	2.982	.468	157.5	- 4.1	.00355	44.1	
	3.084	.689	170.5	-17.9	.00341	49.6	
	3.080	.146	133.9	+ 3.8	.00451	40.5	
	3.127	.351	157.4	+15.8	.00371	45.0	
	3.219	.564	164.4	+15.8	.00355	48.1	
	3.324	.805	188.5	+22.4	.00341	60.7	
	3.240	.199	146.2	+38.7	.00376	40.1	
	3.287	.467	147.2	+23.2	.00324	35.1	
	3.362	.680	159.6	+18.4	.00341	57.8	
	3.461	.937	210.7	+34.0	.00332	73.7	
	3.414	.242	128.5	+36.2	.00376	31.0	
	3.496	.541	161.6	+31.0	.00324	42.3	

TABLE A-IV. (CONTINUED) COMPARISON OF FLOW VECTORS - MODEL V

Time, $\mu\text{sec}$	Position, in.		Flow Speed, ft/sec	Angle, deg	Density, slugs/ft <sup>3</sup>	$q$ , lb/ft <sup>2</sup>	Remarks
x	y						
	3.546	.765	187.7	+36.2	.00341	60.0	
	3.653	1.053	246.8	+40.2	.00332	101.1	
	3.525	.262	103.9	+19.7	.00301	16.3	
	3.606	.579	139.7	+ 9.1	.00381	37.2	
	3.675	.850	196.1	+26.6	.00363	69.7	
	3.798	1.157	242.2	+33.4	.00331	97.1	
	3.684	.304	109.0	+31.8	.00301	17.9	
	3.762	.653	117.6	+42.3	.00381	26.4	
	3.858	.978	167.6	+34.2	.00363	50.9	
	4.002	1.300	242.5	+39.2	.00331	97.4	
685	2.149	.058	78.5	- 9.1	.00451	13.9	
	2.213	.148	89.6	-14.0	.00346	13.9	
	2.329	.262	93.9	-37.6	.00346	15.2	
	2.502	.420	110.9	+ 7.7	.00310	40.1	
	2.538	.096	94.8	-11.0	.00451	20.3	
	2.611	.237	147.6	- 2.5	.00346	37.7	
	2.707	.385	136.8	+ 2.9	.00346	32.4	
	2.850	.602	134.8	-13.2	.00310	28.2	
	2.908	.103	130.6	- 9.5	.00470	40.1	
	2.953	.286	128.4	-10.9	.00355	29.3	
	3.033	.465	119.9	-19.5	.00349	25.1	
	3.140	.671	153.6	+ 8.8	.00340	40.1	
	3.134	.150	116.4	-15.9	.00470	31.8	
	3.210	.374	131.6	- 6.0	.00355	30.8	
	3.290	.584	146.8	- 5.0	.00349	37.6	
	3.407	.839	165.2	+ 6.7	.00340	46.4	
	3.286	.235	147.6	+ 1.3	.00349	38.0	
	3.338	.489	164.2	+16.1	.00343	46.3	
	3.432	.704	160.2	+19.7	.00349	44.8	
	3.528	.982	198.4	+17.2	.00319	62.8	
	3.461	.277	126.5	+14.0	.00349	28.0	
	3.541	.568	110.4	+25.6	.00343	20.9	
	3.620	.820	181.0	+34.4	.00349	57.1	
	3.723	1.113	238.9	+37.7	.00319	91.0	
	3.575	.280	108.4	+ 4.4	.00280	16.4	
	3.651	.586	123.9	+27.9	.00417	32.0	
	3.751	.888	184.4	+35.7	.00428	72.7	
	3.883	1.214	320.2	+40.1	.00331	169.7	
	3.722	.327	94.7	- 4.8	.00280	12.6	
	3.801	.689	119.7	+32.2	.00417	29.9	
	3.903	1.009	259.7	+48.9	.00428	144.2	
	4.120	1.396	330.5	+32.2	.00331	180.7	

TABLE A-IV. (CONTINUED) COMPARISON OF FLOW VECTORS - MODEL V

Time, μsec	Position, in.		Flow Speed, Angle,		Density, <sup>3</sup>	q, <sup>2</sup>	Remarks
	x	y	ft/sec	deg	slugs/ft <sup>3</sup>	lb/ft <sup>2</sup>	
723	2.195	.051	99.5	-15.6	.00507	25.1	
	2.278	.132	93.7	-79.7	.00331	14.5	
	2.376	.226	173.0	+16.5	.00353	52.9	
	2.609	.434	162.5	-65.6	.00316	41.7	
	2.613	.081	137.9	+ 7.9	.00507	48.2	
	2.692	.233	142.1	- 6.1	.00331	33.4	
	2.779	.389	127.5	-20.6	.00353	28.7	
	2.911	.588	161.1	+12.0	.00316	41.0	
	2.915	.096	120.0	+11.0	.00510	36.7	
	3.000	.277	138.1	+10.5	.00348	33.1	
	3.089	.445	157.9	+24.9	.00398	49.6	
	3.221	.684	172.2	+25.3	.00327	48.5	
	3.185	.136	136.4	+14.4	.00510	47.5	
	3.244	.371	127.1	+19.2	.00348	28.1	
	3.351	.579	132.3	+28.9	.00398	34.8	
	3.469	.846	202.2	+36.7	.00327	66.9	
	3.365	.237	103.8	+18.4	.00367	19.8	
	3.432	.516	140.5	+ 9.5	.00407	40.1	
	3.503	.729	186.5	+34.6	.00405	70.4	
	3.628	1.013	226.1	+40.2	.00364	93.0	
	3.519	.291	97.1	+ 3.4	.00367	17.3	
	3.586	.590	138.9	+27.1	.00407	39.2	
	3.684	.863	188.1	+42.8	.00405	71.6	
	3.827	1.192	333.5	+42.2	.00364	202.4	
762	2.240	.038	134.2	- 5.3	.00541	48.7	Vortex has almost destroyed reflection.
	2.282	.112	157.7	- 2.5	.00337	41.9	
	2.473	.255	240.7	-12.8	.00323	93.7	
	2.627	.394	260.8	+11.5	.00339	115.4	
	2.665	.089	137.0	- 7.0	.00541	50.7	
	2.743	.228	120.3	-19.0	.00337	24.4	
	2.822	.375	158.7	- 4.1	.00323	40.8	
	2.996	.606	200.0	0.0	.00339	67.9	
	3.017	.109	160.8	- 3.8	.00439	56.7	
	3.078	.291	156.8	+ 1.6	.00343	42.2	
	3.167	.481	174.3	+ 5.6	.00381	57.8	
	3.290	.716	165.2	+12.4	.00322	43.9	
	3.255	.154	152.4	+ 6.2	.00439	50.9	
	3.322	.398	154.4	+14.0	.00343	40.9	
	3.404	.608	183.0	+25.7	.00381	63.7	
	3.568	.921	247.6	+29.2	.00322	98.6	
	3.582	.242	85.4	-10.0	.00331	12.1	
	3.465	.521	122.0	+19.7	.00342	25.5	
	3.584	.785	156.7	+ 4.4	.00341	41.8	
	3.709	1.082	172.7	+21.4	.00331	49.4	

TABLE A-IV. (CONTINUED) COMPARISON OF FLOW VECTORS - MODEL V

Time, μsec	Position, in.		Flow Speed, ft/sec	Angle, deg	Density, slugs/ft <sup>3</sup>	q, lb/ft <sup>2</sup>	Remarks
	3.550	.293	118.7	+13.1	.00331	23.3	
	3.657	.626	156.9	+18.9	.00342	42.1	
	3.756	.930	204.7	+28.1	.00341	71.4	
	3.961	1.314	315.4	+33.9	.00331	164.6	
800	2.318	.031	103.3	+ 5.7	.00613	32.7	
	2.408	.107	152.6	+20.6	.00398	46.3	
	2.593	.228	151.6	+73.3	.00429	49.3	
	2.822	.434	300.1	+58.8	.00372	167.6	
	2.739	.080	156.1	- 4.4	.00613	74.6	
	2.801	.208	128.1	- 5.4	.00398	32.6	
	2.924	.365	185.2	+14.7	.00429	73.5	
	3.096	.606	161.2	+ 4.1	.00372	48.4	
	3.098	.103	149.3	+13.1	.00468	52.2	
	3.143	.293	115.7	-15.3	.00345	23.1	
	3.241	.488	162.5	+ 8.3	.00374	49.4	
	3.364	.732	189.6	+20.4	.00305	54.8	
	3.322	.161	137.2	+17.9	.00468	44.1	
	3.380	.412	130.5	+ 8.6	.00345	29.4	
	3.501	.655	197.0	+14.4	.00374	72.7	
	3.659	.971	200.7	+23.7	.00305	61.4	
	3.443	.232	139.2	+30.7	.00329	31.9	
	3.541	.548	151.8	+30.4	.00321	36.9	
	3.631	.789	180.1	+40.1	.00325	52.8	
	3.760	1.102	315.1	+45.9	.00271	134.6	
	3.628	.311	159.1	+37.5	.00329	41.6	
	3.720	.648	188.9	+49.7	.00321	57.2	
	3.837	.973	281.8	+52.8	.00325	129.2	
	4.055	1.377	260.2	+37.0	.00271	91.8	
838	3.152	.116	143.3	+ 2.7	.00406	41.7	Vortex has become indistinct.
	3.183	.282	167.0	+14.9	.00358	49.9	
	3.315	.499	164.7	+ 6.8	.00368	49.9	
	3.456	.767	190.5	+ 8.1	.00308	55.9	
	3.378	.179	168.1	+15.4	.00406	57.3	
	3.440	.421	169.5	+18.8	.00358	51.4	
	3.572	.673	236.3	+31.7	.00368	102.7	
	3.733	1.004	257.0	+39.8	.00308	101.9	
876	3.228	.119	132.0	+ 4.6	.00398	34.7	
	3.291	.311	157.7	+ 6.3	.00348	43.3	
	3.391	.508	140.5	+22.2	.00348	34.3	
	3.532	.778	183.3	+36.2	.00273	46.0	
	3.471	.204	124.1	-11.3	.00398	30.6	

TABLE A-IV. (CONTINUED) COMPARISON OF FLOW VECTORS - MODEL V

Time, $\mu$ sec	Position, in.		Flow Speed, ft/sec	Angle, deg	Density, <sup>3</sup> slugs/ft <sup>3</sup>	q, lb/ft <sup>2</sup>	Remarks
x	y						
	3.530	.452	167.2	+25.8	.00348	48.7	
	3.695	.749	185.0	+45.0	.00348	59.5	
	3.852	1.103	286.2	+55.2	.00273	112.0	
914	3.273	.123	118.0	+13.2	.00407	28.4	
	3.324	.315	88.7	- 2.1	.00342	13.5	
	3.440	.528	121.7	+31.3	.00345	25.5	
	3.606	.832	187.2	+31.2	.00296	52.0	
	3.489	.201	61.4	+ 2.7	.00407	7.7	
	3.583	.477	113.5	+25.6	.00342	22.0	
	3.713	.767	166.9	+45.0	.00345	48.0	
	3.914	1.192	278.2	+32.5	.00296	114.7	

# DISTRIBUTION LIST

<u>No. of Copies</u>	<u>Organization</u>	<u>No. of Copies</u>	<u>Organization</u>
10	Commander Armed Services Technical Information Agency ATTN: TIPCR Arlington Hall Station Arlington 12, Virginia	3	Commanding Officer Picatinny Arsenal ATTN: Library Dover, New Jersey
1	Director of Defense Research and Engineering (OSD) Washington 25, D.C.	1	Commanding Officer Harry Diamond Laboratories ATTN: Technical Information Office, Branch 012 Washington 25, D.C.
1	Director Defense Research and Engineering ATTN: Technical Library Washington 25, D.C.	1	Commanding Officer Harry Diamond Laboratories Washington 25, D.C.
15	Chief, Defense Atomic Support Agency Washington 25, D.C.	1	Research Analysis Corporation ATTN: Document Control Office 6935 Arlington Road Bethesda, Maryland Washington 14, D.C.
2	Commanding General Field Command Defense Atomic Support Agency ATTN: Training Division Sandia Base P. O. Box 5100 Albuquerque, New Mexico	1	U.S. Documents Officer U.S. National Military Representative SHAPE APO 55, New York, New York
1	Commandant Armed Forces Staff College ATTN: Secretary Norfolk 11, Virginia	1	Commanding General U.S. Army Chemical Corps R and D Command Washington 25, D.C.
1	Director IDA/Weapons Systems Evaluation Group Room 1J875, The Pentagon Washington 25, D.C.	1	Commanding Officer U.S. Army Chemical Warfare Laboratories Edgewood Arsenal, Maryland
2	Commanding General U.S. Army Material Command ATTN: AMCRD-RS-PE-Bal AMCRD-DE-N Research and Development Directorate Washington 25, D.C.	2	Chief of Engineers Building T7, Gravelly Point Department of the Army Washington 25, D.C.

# DISTRIBUTION LIST

<u>No. of Copies</u>	<u>Organization</u>	<u>No. of Copies</u>	<u>Organization</u>
1	Commanding General Engineering Research and Development Laboratories ATTN: Chief, Technical Intelligence Branch U.S. Army Fort Belvoir, Virginia	1	Commanding General U.S. Army Continental Command Fort Monroe, Virginia
1	Commandant U.S. Army Engineers School Fort Belvoir, Virginia	1	Commanding General U.S. Army Combat Development Agency Fort Belvoir, Virginia
1	Director Waterways Experiment Station ATTN: Library Vicksburg, Mississippi	1	President U.S. Army Air Defense Board Fort Bliss, Texas
1	Commanding General U.S. Army Signal Research and Development Laboratory ATTN: Technical Documents Center, Evans Area Fort Monmouth, New Jersey	1	Commandant U.S. Army Air Defense School ATTN: Command and Staff Department Fort Bliss, Texas
2	Commanding Officer U.S. Army Signal Missile Support Agency ATTN: SIGWS-RD-MM White Sands Missile Range New Mexico	1	Commanding Officer Office of Special Weapons Development Fort Bliss 16, Texas
2	Commanding General White Sands Missile Range ATTN: Technical Library New Mexico	1	Commandant Army War College ATTN: Library Carlisle Barracks, Pennsylvania
1	Commanding Officer U.S. Army Transportation Research Command ATTN: Chief, Technical Information Division Fort Eustis, Virginia	1	Chief of Research and Development ATTN: Director/Special Weapons Atomic Division Department of the Army Washington 25, D.C.
		3	Chief, Bureau of Naval Weapons ATTN: DIS-33 Department of the Navy Washington 25, D.C.
		3	Chief of Naval Operations Department of the Navy Washington 25, D.C.



# DISTRIBUTION LIST

<u>No. of Copies</u>	<u>Organization</u>	<u>No. of Copies</u>	<u>Organization</u>
1	Chief of Naval Research ATTN: Code 811 Department of the Navy Washington 25, D.C.	1	Commander U.S. Naval Ordnance Test Station ATTN: Technical Library China Lake, California
2	Chief, Bureau of Ships ATTN: Code 348 Code 423 Department of the Navy Washington 25, D.C.	5	Commander Naval Ordnance Laboratory ATTN: Explosives Department White Oak Silver Spring 19, Maryland
3	Chief, Bureau of Yards and Docks ATTN: Code P-300 D-400 D-440 Department of the Navy Washington 25, D.C.	1	Commanding Officer and Director U.S. Naval Radiological Defense Laboratory ATTN: Technical Information Agency San Francisco 24, California
1	Commanding Officer and Director David W. Taylor Model Basin ATTN: Aerodynamics Laboratory Washington 7, D.C.	1	Director U.S. Naval Research Laboratory Washington 25, D.C.
1	Commanding Officer and Director U.S. Navy Electronics Laboratory ATTN: Code 4223 San Diego 52, California	1	Superintendent U.S. Naval Postgraduate School Monterey, California
1	Commanding Officer U.S. Damage Control Training Center ATTN: ABC Defense Course Naval Base Philadelphia, Pennsylvania	1	Commanding Officer U.S. Naval Schools Command U.S. Naval Station Treasure Island San Francisco, California
1	Director of Naval Intelligence ATTN: OP-922V Department of the Navy Washington 25, D.C.	1	Officer In Charge U.S. Naval School Civil Engineer Corps Officers ATTN: Code 753 U.S. Naval Construction Battalion Center Port Hueneme, California
1	Commander Norfolk Naval Shipyard ATTN: Code 270 Portsmouth, Virginia	1	Commanding Officer U.S. Naval Weapons Evaluation Facility ATTN: Code 42 Kirtland Air Force Base Albuquerque, New Mexico

# DISTRIBUTION LIST

<u>No. of Copies</u>	<u>Organization</u>	<u>No. of Copies</u>	<u>Organization</u>
1	President U.S. Naval War College Newport, Rhode Island	4	Commandant U.S. Marine Corps ATTN: Code AO3H Washington 25, D.C.
1	Commander-in-Chief U.S. Atlantic Fleet U.S. Naval Base Norfolk 11, Virginia	1	Commander Space Systems Division A.F. Unit Post Office Los Angeles 45, California
1	Commander-in-Chief U.S. Pacific Fleet FPO, San Francisco, California	1	Commander Air Force Systems Command Andrews Air Force Base Washington 25, D.C.
1	Commanding Officer U.S. Fleet Training Center ATTN: Special Weapons School Naval Station Norfolk 11, Virginia	3	Commander Air Force Cambridge Research Laboratory ATTN: CRED L. G. Hanscom Field Bedford, Massachusetts
2	Commanding Officer U.S. Fleet Training Center ATTN: SPWP School Naval Station San Diego, California	1	Commander Air Force Special Weapons Center ATTN: Library Kirtland Air Force Base New Mexico
1	Commanding Officer Nuclear Weapons Training Center, Atlantic ATTN: Nuclear Warfare Department U.S. Naval Base Norfolk 11, Virginia	1	Commander Tactical Air Command ATTN: Document Security Branch Langley Air Force Base Langley Field, Virginia
2	Commanding Officer Nuclear Weapons Training Center, Pacific U.S. Naval Air Station North Island San Diego 35, California	2	Director Air University Library ATTN: (3T-AUL-60-118) Maxwell Air Force Base Ohio
1	Commanding Officer U.S. Naval Unit Chemical Corps School Army Chemical Training Center Fort McClellan, Alabama	1	Commander-in-Chief Strategic Air Command ATTN: Special Weapons Branch Inspector Division Inspector General Offutt Air Force Base, Nebraska

# DISTRIBUTION LIST

<u>No. of Copies</u>	<u>Organization</u>	<u>No. of Copies</u>	<u>Organization</u>
1	Commander Aeronautical Systems Division Wright-Patterson Air Force Base Ohio	2	Director of Research and Technology U.S. Air Force ATTN: Chief, Research Division Combat Components Division Washington 25, D.C.
1	Commander Air Force Logistics Command Wright-Patterson Air Force Base Ohio	2	Director, Project RAND Department of the Air Force 1700 Main Street Santa Monica, California
1	Commandant U.S. Air Force Institute of Technology ATTN: Resident College Wright-Patterson Air Force Base Ohio	1	Manager Albuquerque Operations U.S. Atomic Energy Commission P. O. Box 5400 Albuquerque, New Mexico
1	Assistant for Atomic Energy U.S. Air Force Washington 25, D.C.	2	U.S. Atomic Energy Commission Technical Information Service 1901 Constitution Avenue, N.W. Washington 25, D.C.
1	Headquarters U.S. Air Force AFTAC Washington 25, D.C.	2	U.S. Atomic Energy Commission Los Alamos Scientific Laboratory ATTN: Report Librarian P. O. Box 1663 Los Alamos, New Mexico
1	Special Assistant for Installations U.S. Air Force ATTN: AFCIE-E Washington 25, D.C.	1	Director National Aeronautics and Space Administration ATTN: Mr. Eugene B. Jackson - Chief, Division of Research Information 1520 H Street, N.W. Washington 25, D.C.
1	Director of Intelligence U.S. Air Force ATTN: AFOIN-1B2 Washington 25, D.C.	2	Director National Aeronautics and Space Administration ATTN: Mr. John Stack Library Langley Research Center Langley Field, Virginia
1	Director of Plans U.S. Air Force ATTN: War Plans Division Washington 25, D.C.		
1	Director of Requirements U.S. Air Force ATTN: AFDRQ-SA/M Washington 25, D.C.		

# DISTRIBUTION LIST

<u>No. of Copies</u>	<u>Organization</u>	<u>No. of Copies</u>	<u>Organization</u>
1	Forest Service U.S. Department of Agriculture ATTN: Mr. A. A. Brown Chief, Division of Forest Fire Research Washington 25, D.C.	1	Rensselaer Polytechnic Institute ATTN: Dr. Clayton Oliver Dobrenwend Mason House Troy, New York
1	Armour Research Foundation Illinois Institute of Technology Center ATTN: Dr. S. J. Fraenkel Division of Engineering Mechanics Chicago 16, Illinois	1	University of Michigan University Research Office ATTN: Dr. B. Johnson Lobby 1, East Engineering Bldg. Ann Arbor, Michigan
1	Broadview Research Corporation ATTN: Dr. Richard I. Condit P. O. Box 1093 Burlingame, California	1	Dr. Walker Bleakney Palmer Physical Laboratory Princeton University Princeton, New Jersey
1	Edgevton, Germeshausen and Grier, Inc. ATTN: D. F. Hansen Boston, Massachusetts	1	Dr. Otto Laporte Engineering Research Institute University of Michigan Ann Arbor, Michigan
3	President Sandia Corporation ATTN: Dr. E. Cox, Physics Division Dr. J. Shreve, Blast Model Studies Division Dr. Walter A. MacNair Sandia Base Albuquerque, New Mexico	1	Dr. N. M. Newmark Illinois Talbot Laboratory University of Illinois Urbana, Illinois
1	Applied Physics Laboratory The Johns Hopkins University 8621 Georgia Avenue Silver Spring, Maryland	10	The Scientific Information Office Defence Research Staff British Embassy 3100 Massachusetts Avenue, N.W. Washington 8, D.C.
1	Massachusetts Institute of Technology ATTN: Dr. R. J. Hansen Cambridge 39, Massachusetts	4	Defence Research Member Canadian Joint Staff ATTN: Canadian Army Staff 2450 Massachusetts Avenue, N.W. Washington 8, D.C.

<p>AD _____ Accession No. _____</p> <p>Ballistic Research Laboratories, AFG</p> <p>DESIGN OF AIRCRAFT REVETMENTS</p> <p>G. A. Coulter and R. L. Peterson</p> <p>BRL Memorandum Report No. 1440 October 1962</p> <p>UNCLASSIFIED Report</p>	<p>UNCLASSIFIED</p> <p>Airplanes -</p> <p>Blast effects</p> <p>Ground protection -</p> <p>Aircraft</p>	<p>Air flow over two-dimensional model revetments, mounted in the 4 x 15 Inch Shock Tube, was traced by means of cigarette smoke grids photographed by a high speed framing camera. Tables of densities, flow speeds, and directions of flow, computed from the photographs, are given for an input shock wave of 8.3 psi average overpressure. Flow vectors are shown to illustrate the differences in the flow patterns for the different revetments tested.</p>
<p>AD _____ Accession No. _____</p> <p>Ballistic Research Laboratories, AFG</p> <p>DESIGN OF AIRCRAFT REVETMENTS</p> <p>G. A. Coulter and R. L. Peterson</p> <p>BRL Memorandum Report No. 1440 October 1962</p> <p>UNCLASSIFIED Report</p>	<p>UNCLASSIFIED</p> <p>Airplanes -</p> <p>Blast effects</p> <p>Ground protection -</p> <p>Aircraft</p>	<p>Air flow over two-dimensional model revetments, mounted in the 4 x 15 Inch Shock Tube, was traced by means of cigarette smoke grids photographed by a high speed framing camera. Tables of densities, flow speeds, and directions of flow, computed from the photographs, are given for an input shock wave of 8.3 psi average overpressure. Flow vectors are shown to illustrate the differences in the flow patterns for the different revetments tested.</p>
<p>AD _____ Accession No. _____</p> <p>Ballistic Research Laboratories, AFG</p> <p>DESIGN OF AIRCRAFT REVETMENTS</p> <p>G. A. Coulter and R. L. Peterson</p> <p>BRL Memorandum Report No. 1440 October 1962</p> <p>UNCLASSIFIED Report</p>	<p>UNCLASSIFIED</p> <p>Airplanes -</p> <p>Blast effects</p> <p>Ground protection -</p> <p>Aircraft</p>	<p>Air flow over two-dimensional model revetments, mounted in the 4 x 15 Inch Shock Tube, was traced by means of cigarette smoke grids photographed by a high speed framing camera. Tables of densities, flow speeds, and directions of flow, computed from the photographs, are given for an input shock wave of 8.3 psi average overpressure. Flow vectors are shown to illustrate the differences in the flow patterns for the different revetments tested.</p>
<p>AD _____ Accession No. _____</p> <p>Ballistic Research Laboratories, AFG</p> <p>DESIGN OF AIRCRAFT REVETMENTS</p> <p>G. A. Coulter and R. L. Peterson</p> <p>BRL Memorandum Report No. 1440 October 1962</p> <p>UNCLASSIFIED Report</p>	<p>UNCLASSIFIED</p> <p>Airplanes -</p> <p>Blast effects</p> <p>Ground protection -</p> <p>Aircraft</p>	<p>Air flow over two-dimensional model revetments, mounted in the 4 x 15 Inch Shock Tube, was traced by means of cigarette smoke grids photographed by a high speed framing camera. Tables of densities, flow speeds, and directions of flow, computed from the photographs, are given for an input shock wave of 8.3 psi average overpressure. Flow vectors are shown to illustrate the differences in the flow patterns for the different revetments tested.</p>